

# Nonlinear-based MEMS sensors and active switches for gas and acceleration applications



**Mohammad Younis**

*Mechanical Engineering*



The 3rd International Electronic Conference on Sensors and Applications

# Outline

- Part I: Gas Sensing and Switches

- Jump-up and jump down switches (with controllers)

- Pull-in based switches (without controllers)

- Summary and Conclusions Part I

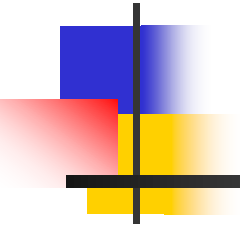
- Part II: Acceleration Triggers and Switches

- Moderate Acceleration

- Low-g

- Summary and Conclusions Part II

# Part I: Gas



# Historical Background

TRANSACTIONS ON ELECTRON DEVICES, VOL. ED-33, NO. 4, APRIL 1986

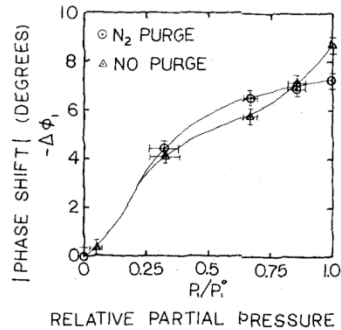


Fig. 12. Equilibrium phase shift as a function of relative xylene partial pressure, with and without purging in nitrogen after each measurement.

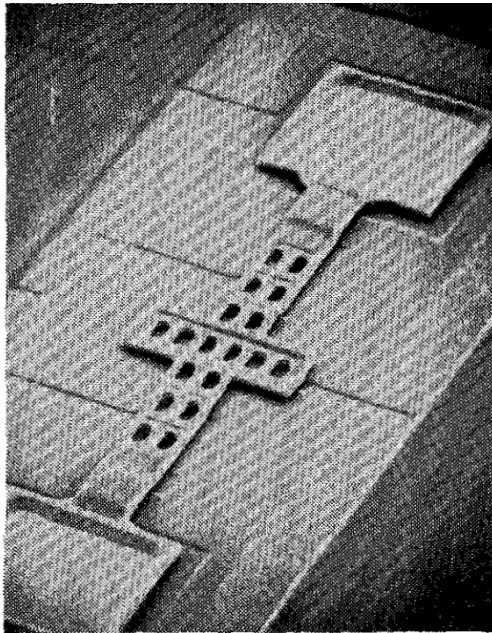


Fig. 7. SEM of type B microbridge with apertures.

Howe and Muller, 1986.

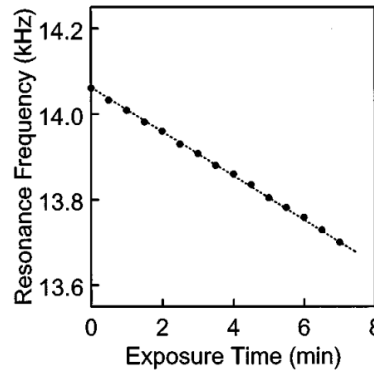


FIG. 1. Frequency response of a silicon nitride cantilever with one side partially covered with evaporated gold. The frequency decreases with exposure time indicating mass loading due to mercury adsorption on the gold coating.

Thundat et al., 1995.

“Detection of mercury vapor using resonating microcantilevers”

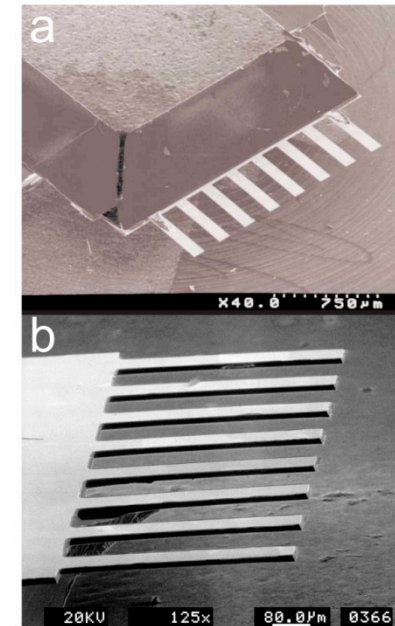


Fig. 2. a Scanning electron microscopy image of a type A micromechanical sensor array with eight sensors (500 μm long, 100 μm wide and 0.8 μm thick). The pitch is 250 μm. Such arrays are suitable for parallel and differential readout in the static measuring mode. b Type B sensor array with the same length and width as above, but a thickness of 12 μm. The greater stiffness of the sensors is suitable for the dynamic measuring mode

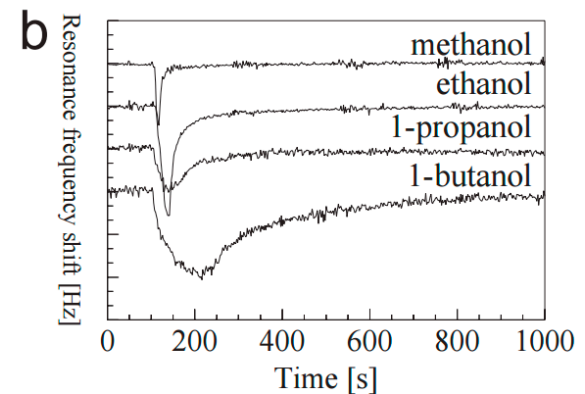


Fig. 4. a Response of a single PMMA-coated sensor :

Lang, et al., “A chemical sensor based on a micromechanical cantilever array for the identification of gases and vapors. Applied Physics A.

# Bifurcation-Based Mass Sensors

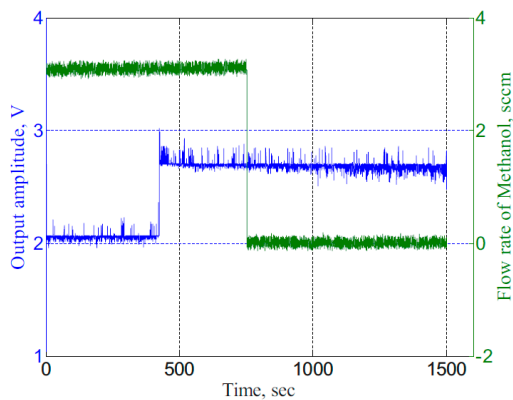
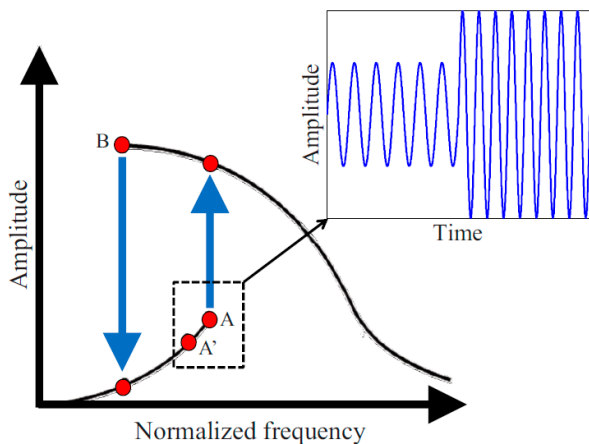
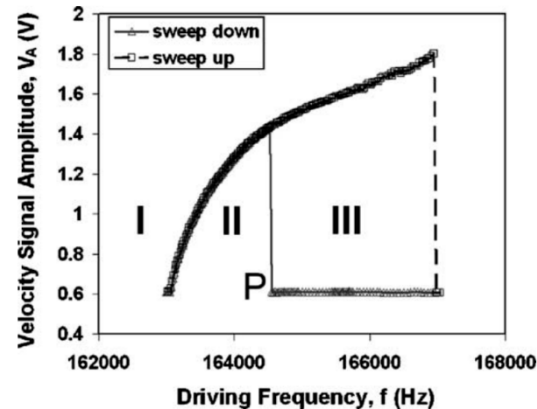


FIG. 6. (Color online) The sensor's response amplitude plotted as a function of time. As the target analyte is added, the bifurcation frequency decreases rendering a sudden jump in response amplitude. This jump in amplitude signals a detection event.



Bifurcation-based mass sensing using piezoelectrically-actuated microcantilevers  
Kumar et al., APL, 2011



$f = (1/2\pi)\sqrt{(4k + 2r_1 V_A^2)/m}$ , where  $k$ ,  $m$ ,  $V_A$  and  $r_1$  are stiffness, mass, driving voltage amplitude applied, and the coefficient of electrostatic force, respectively. A small mass change ( $\Delta m$ ) in the oscillator causes this "jump" frequency to shift ( $\Delta f$ ). Therefore, by measuring the frequency shift, this mass change can be determined by  $|\Delta m| \approx 2m(|\Delta f|/f_0)$ .

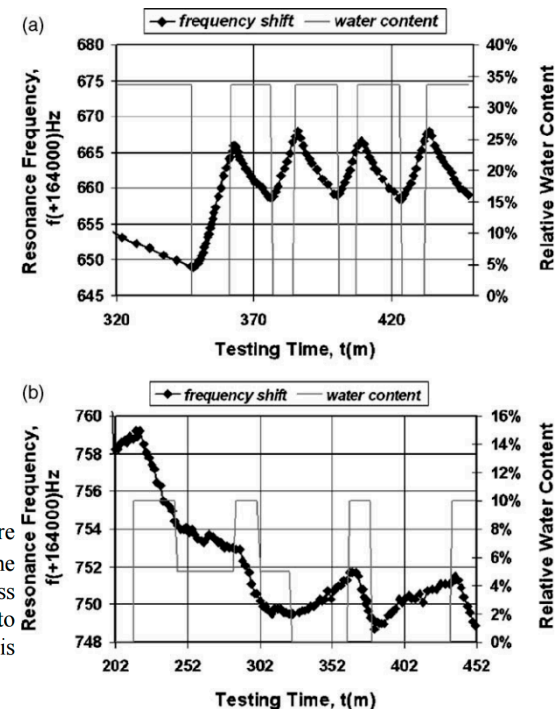


Fig. 12. Frequency shifts at the right side of the first parametric resonance as adjusting water content in the testing chamber.

Zhang and Turner, Sensors and Actuators A: Physical  
Volume 122, Issue 1, 29 July 2005, Pages 23–30  
Application of parametric resonance amplification in a single-crystal silicon micro-oscillator based mass sensor

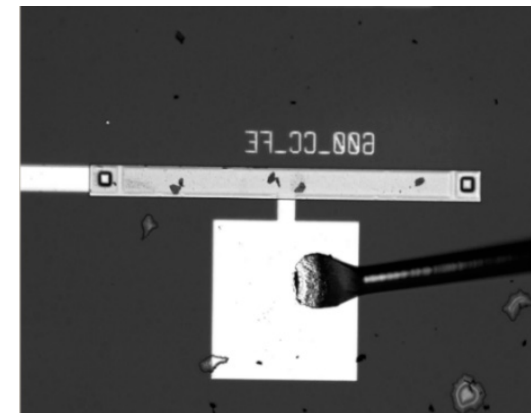
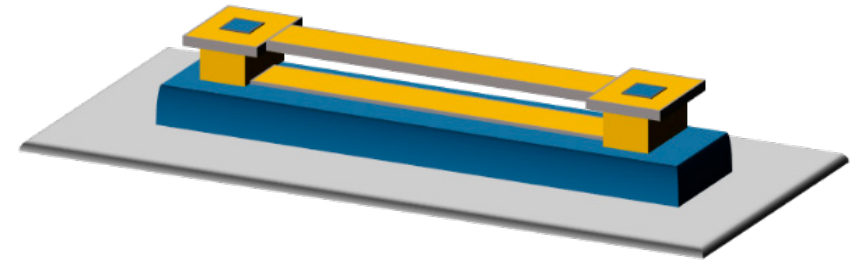
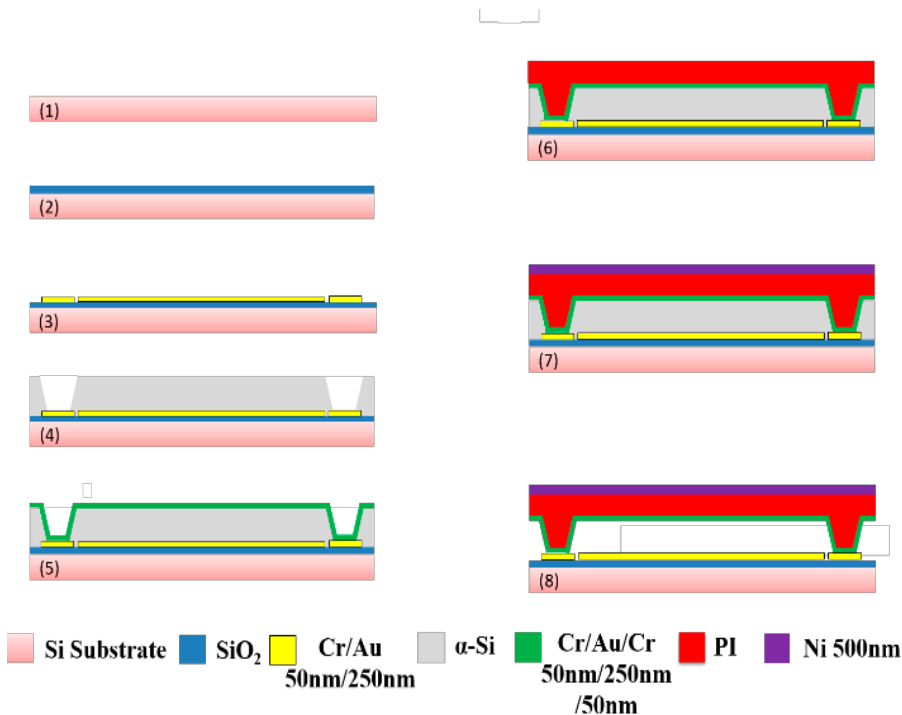
# Objective

- ❑ There is an increasing interest to realize smarter sensors and actuators that can deliver a multitude of sophisticated functionalities while being compact in size and of low cost.
- ❑ We report here combining both sensing and actuation on the same device based on a single microstructure. Specifically, we demonstrate a smart resonant gas (mass) sensor, which in addition to being capable of quantifying the amount of absorbed gas; can be autonomously triggered as an electrical switch upon exceeding a preset threshold of absorbed gas.
- ❑ We integrate a Metal-Organic Framework MOF thin film.

# Part I: Programmable Switch

- The softening and hardening nonlinear behaviors of the microbeams are exploited to demonstrate the ideas.
- For gas sensing, an amplitude-based tracking algorithm is developed to quantify the captured quantity of gas.
- Then, a MEMS switch triggered by gas using the nonlinear response of the microbeam is demonstrated.
- The proposed switch is promising for delivering binary sensing information, and also can be used directly to activate useful functionalities, such as alarming.

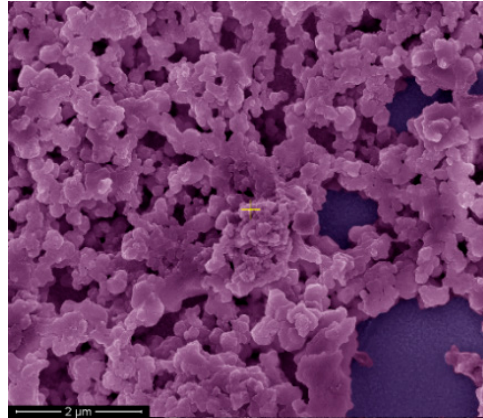
# Fabrication



- Lower electrode, composed of gold/chrome
- Amorphous silicon sacrificial layer
- Structural layer made of polyimide (PI) and metal on top.

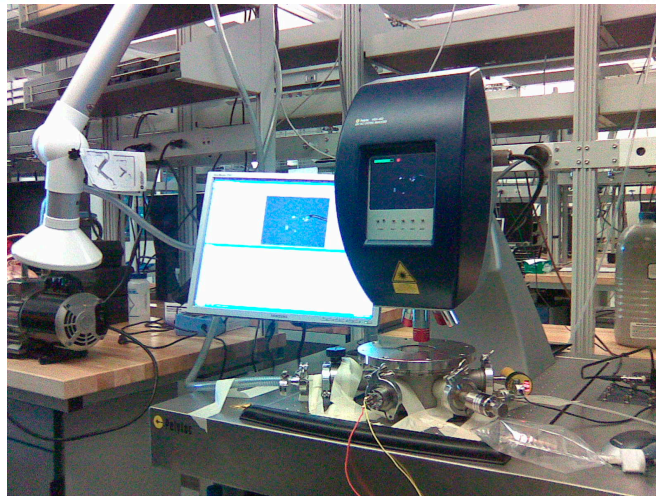
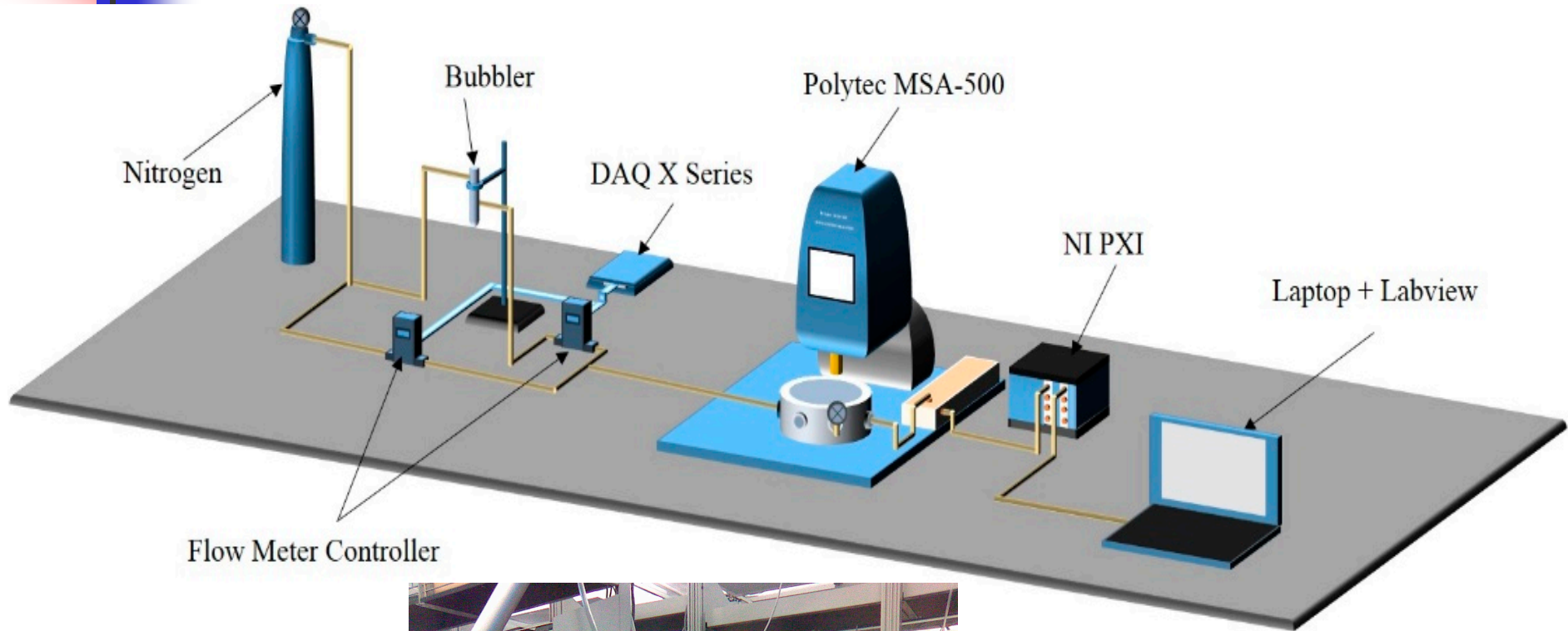
Symbol	Quantity	Dimensions
$L$	Length	600 $\mu\text{m}$
$h$	Thickness	6.85 $\mu\text{m}$
$b$	Width	50 $\mu\text{m}$
$d$	Gap	2 $\mu\text{m}$

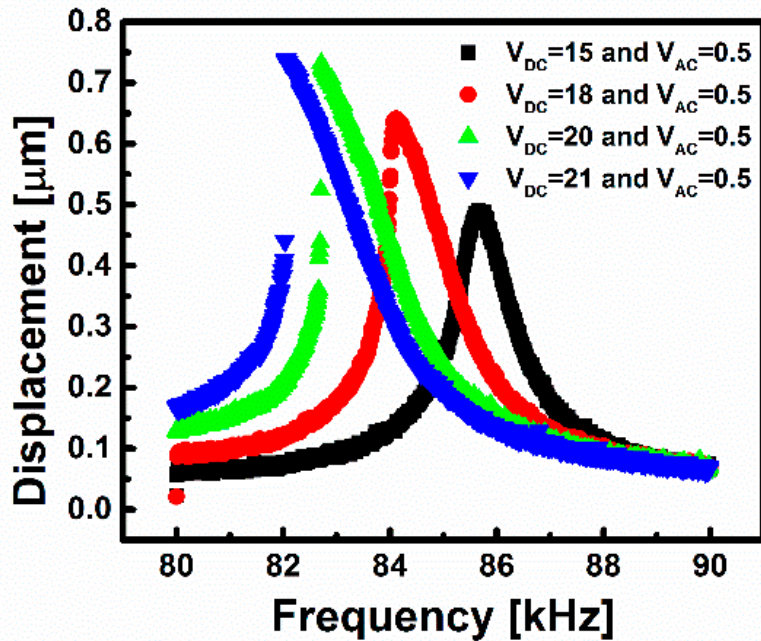
# MOF Coating



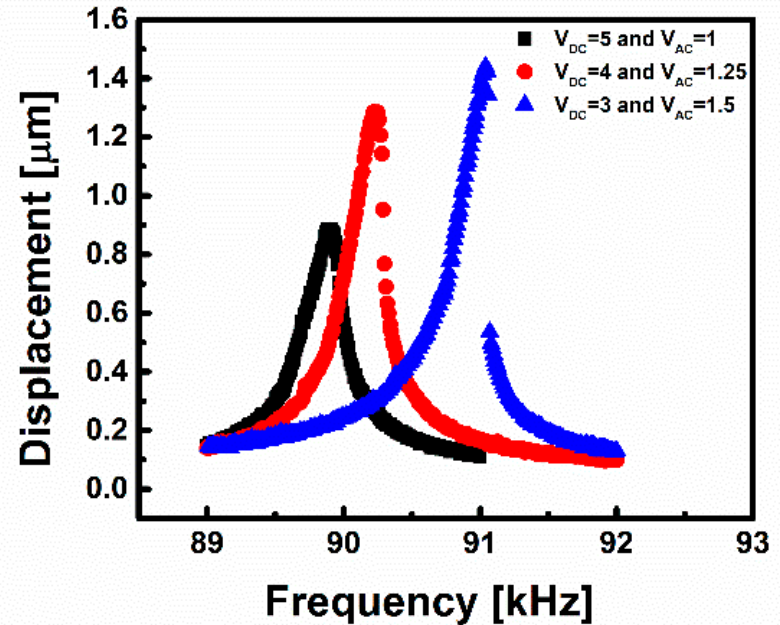
- Metal-Organic Framework MOFs are very promising porous materials for gas sensing applications
- The clamped-clamped microbeam was coated with a MOF thin film using an inkjet printer using a nozzle with 20 μm of diameter.
- We used  $\text{Cu}_3(\text{btc})_2 \cdot x\text{H}_2\text{O}$  MOF (btc is 1, 3, 5-benzenetricarboxylate), also known as HKUST-1.

# Setup





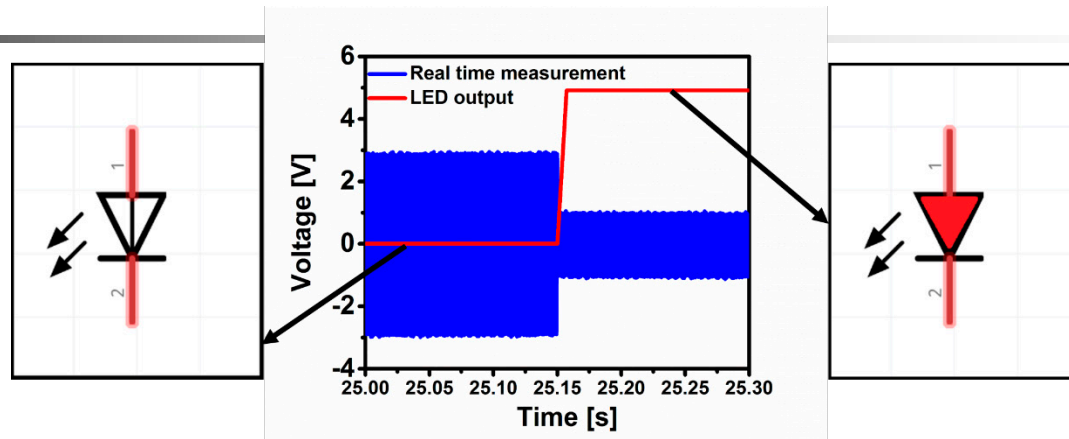
(a)



(b)

- (a) For different DC voltages showing a transition from a linear to a softening behavior at 3.3 Torr, and (b) for different AC voltages showing the transition from linear to hardening behavior at 220 mTorr.

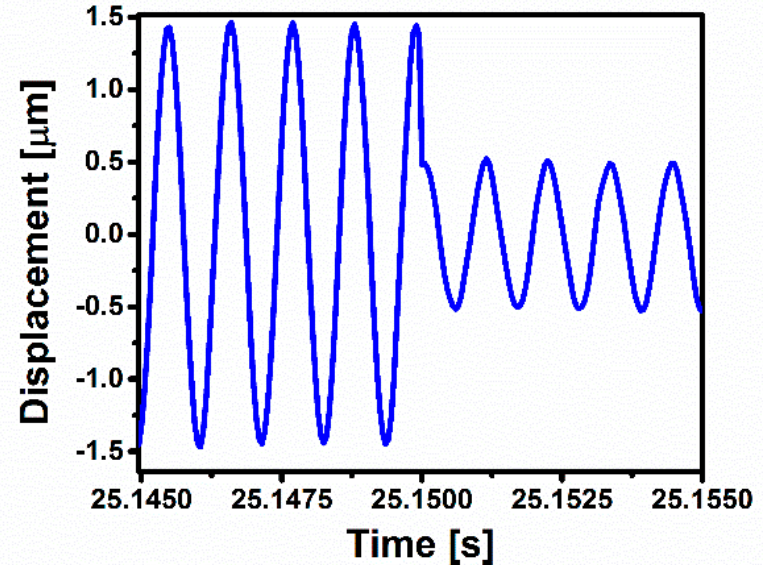
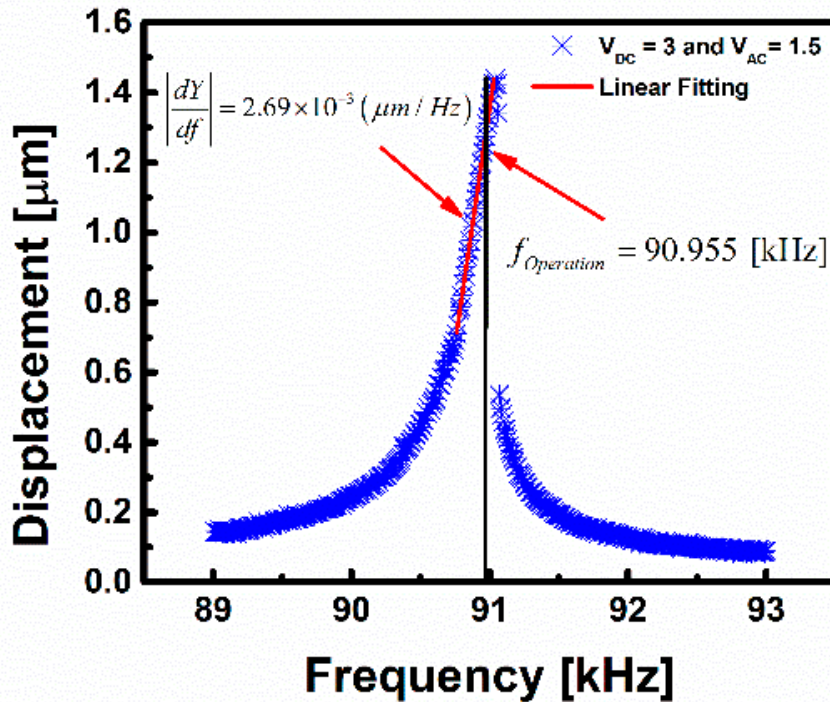
# Jump-Down Sensor and Switch



Time history of the sensor to trigger a LED upon water vapor exposure.

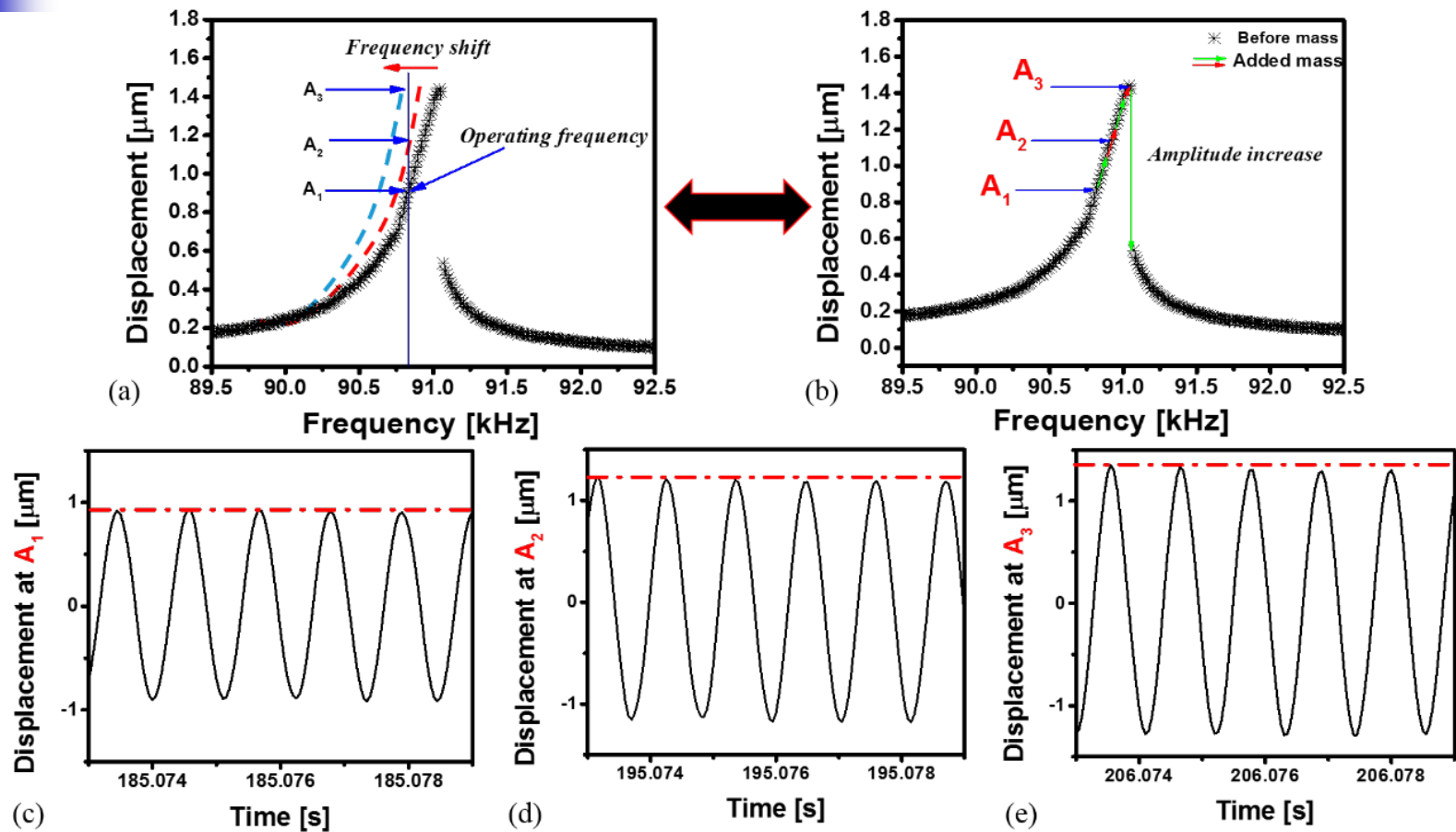
- The outcome from the DAQ is connected to a microprocessor from Arduino .
- A Labview program with an Arduino library is developed in order to read the voltage coming from the laser Doppler controller at a fixed frequency.
- The algorithm is based on calculating the amplitude difference between two successive points during a frequency sweep. When the absolute value of the difference between the current and previous data point exceeds a defined constant, switching is triggered.
- A LED is connected to the Arduino digital output in order to indicate the switching.

# Jump-Down Sensor and Switch



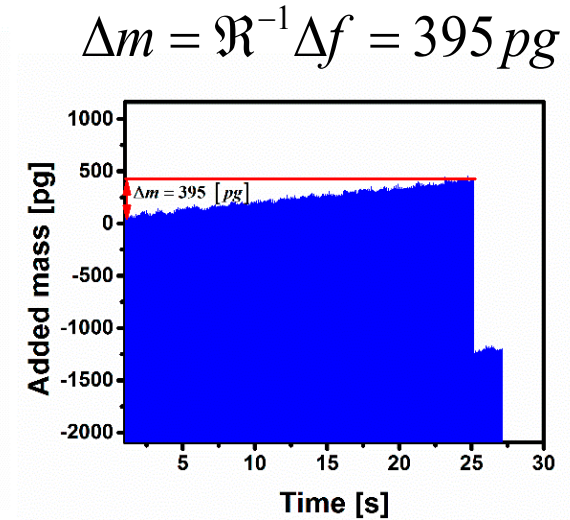
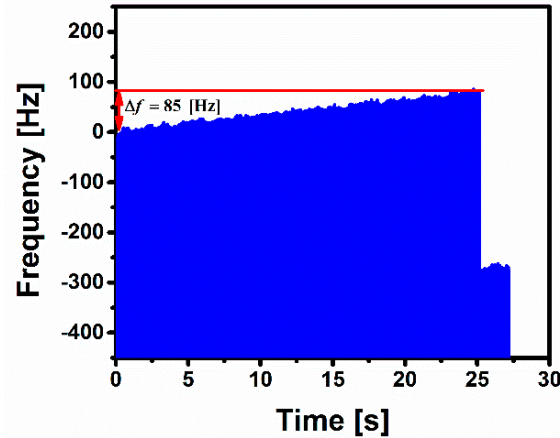
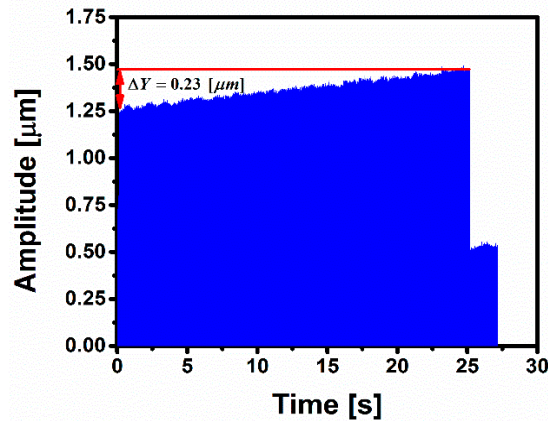
- The linearly-fitted curve can be used to relate the amplitude change to the frequency shift, and hence, the amount of absorbed mass.
- Time history of the beam displacement upon gas exposure indicating the sudden jump down, and hence, the switching event.

# Jump-Down Sensor and Switch



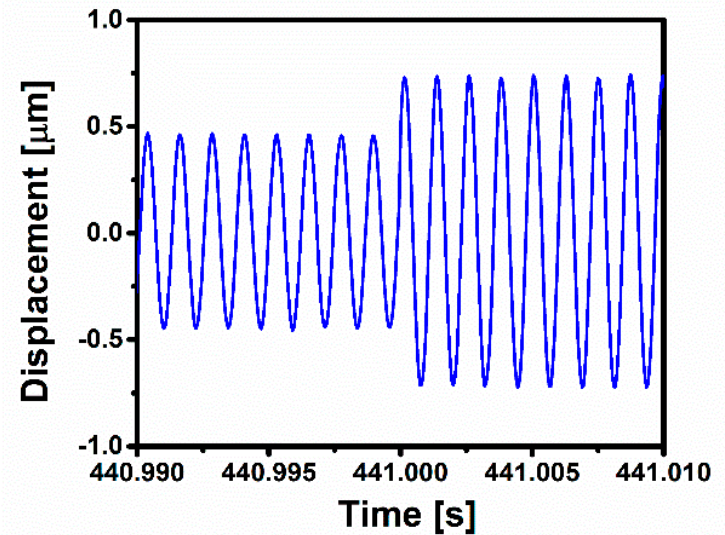
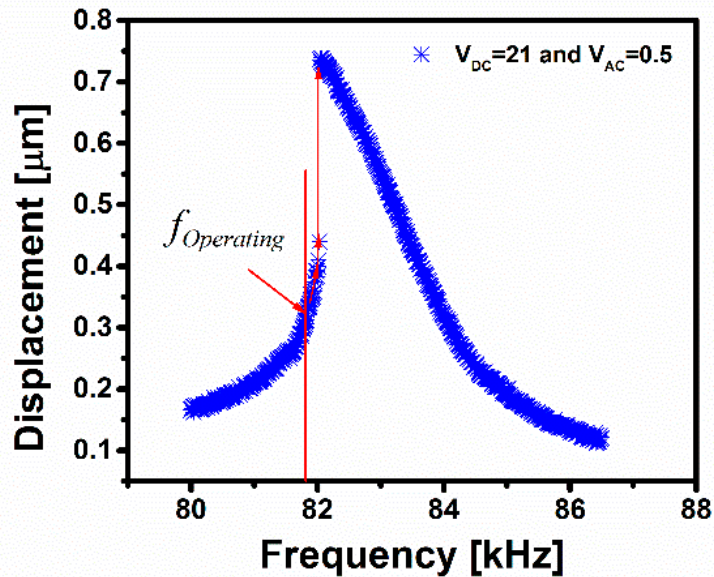
- The vertical line indicates a fixed operating frequency of the resonator during vapor exposure.
- Clearly, the amplitude of the resonator increases with the absorption of vapor.
- Measured time history showing the displacement at (c) point  $A_1$ , (d) point  $A_2$  and (e) point  $A_3$ .

# Jump-Down Sensor and Switch



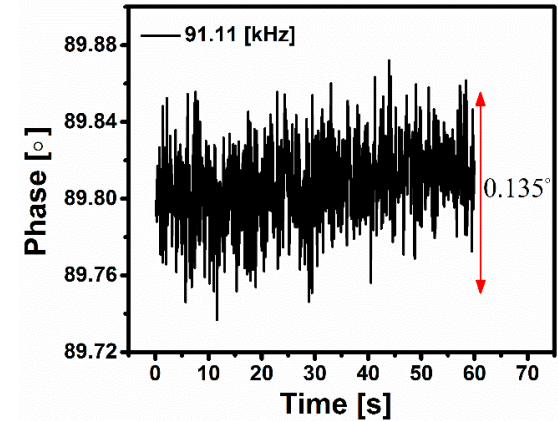
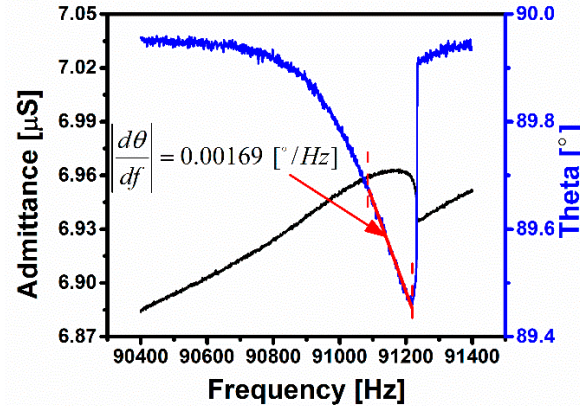
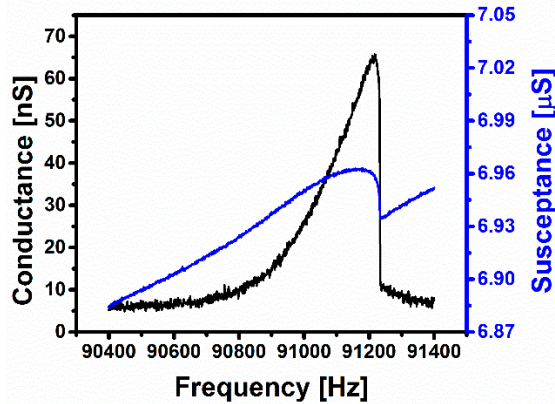
- The calculated slope is used to determine the frequency shift as a function of time.
- Measuring the frequency shift as a function of time, we found  $\Delta f = 85 \text{ Hz}$  before reaching the jump zone.
- The frequency shift coming from the real time measurement  $\Delta f = 85.55 \text{ Hz}$  is very close to the calculated frequency shift using linear fitting.

# Jump-up Switch Triggered by Gas



- Frequency response for the Jump-up switch indicating in the vertical red line the operating point of the device prior to mass detection. The red line highlights the jump in the response from the lower to the upper branches, which occurs upon mass detection when exceeding a certain threshold.
- Time history of the beam displacement upon gas exposure showing the jump from the lower to the upper dynamical states, thereby triggering the switching event.

# Noise Analysis



$V_{DC} = 3V$  and  $V_{AC} = 1V$  and at a pressure of 220 mTorr. (a) Conductance and susceptance as a function of the frequency near resonance. (b) Admittance and phase as a function of the frequency near resonance. (c) Variation of the phase in time at  $f = 91.11 \text{ kHz}$ .

- The frequency shift due to thermal fluctuations around the resonator can be related to the phase variation at a given frequency.
- A precision impedance analyzer connected to a PC with National Instruments data acquisition has been used to characterize the microbeam electrically.

# Noise Analysis

The phase evolution as a function of time at a fixed frequency has been shown. The phase noise has been calculated to be  $d\phi = 0.135^\circ$

, which leads to a frequency shift  $\delta f_{noise} = d\phi / |d\phi / df| = 79.88 \text{ Hz}$

The responsivity of the sensor, which can be expressed as

$$\mathfrak{R}^{-1} = \left| \frac{dm}{df} \right| = \frac{2m_{eff}}{f_{res,0V}} \quad m_{eff} = \alpha m$$

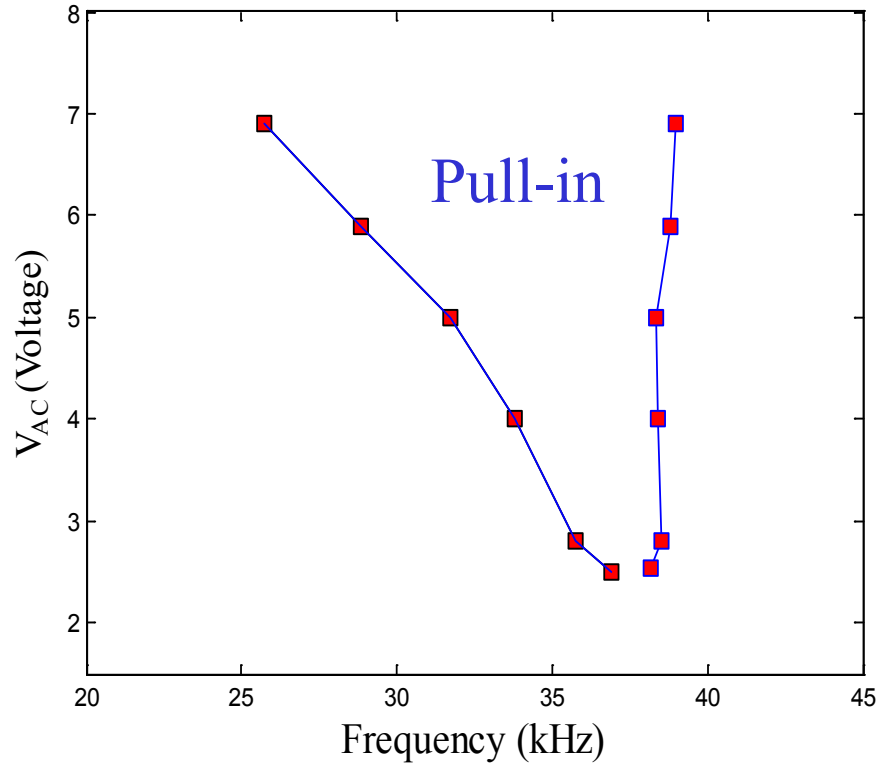
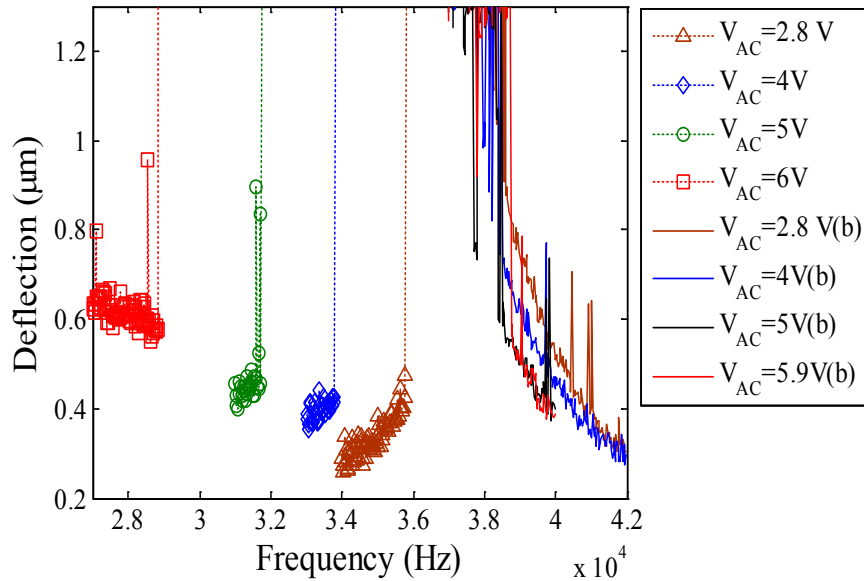
where  $f_{res,0V} = 86.8 \text{ kHz}$  is the natural resonant frequency at  $V_{DC} = 0V$  and

$$\mathfrak{R}_{1st}^{-1} = 4.65 \text{ pg} / \text{ Hz}$$

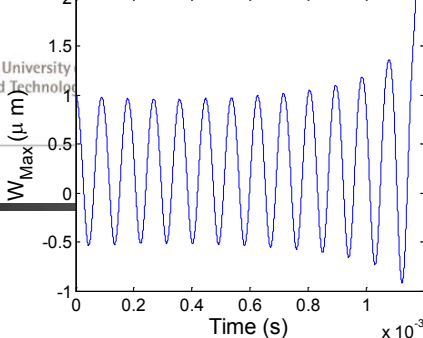
$$\delta m_{noise} = \mathfrak{R}^{-1} \delta f_{noise}$$

$$\delta m_{noise} = 371.442 \text{ pg}$$

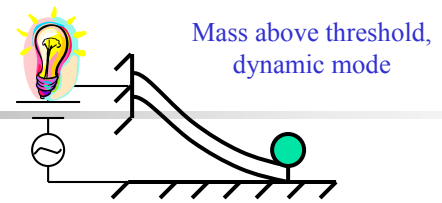
# Can we do it without an algorithm, controller?



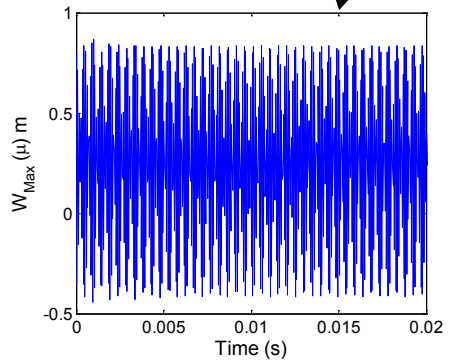
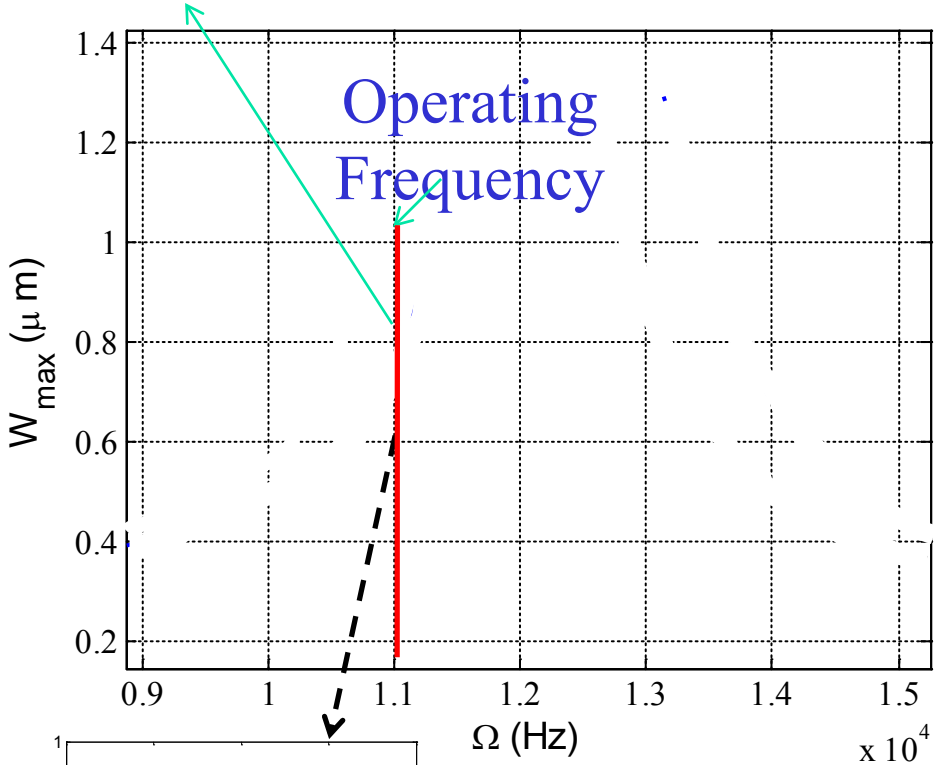
- Yes through dynamic pull-in



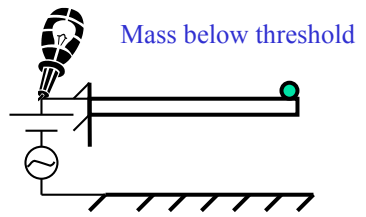
After  
Mass



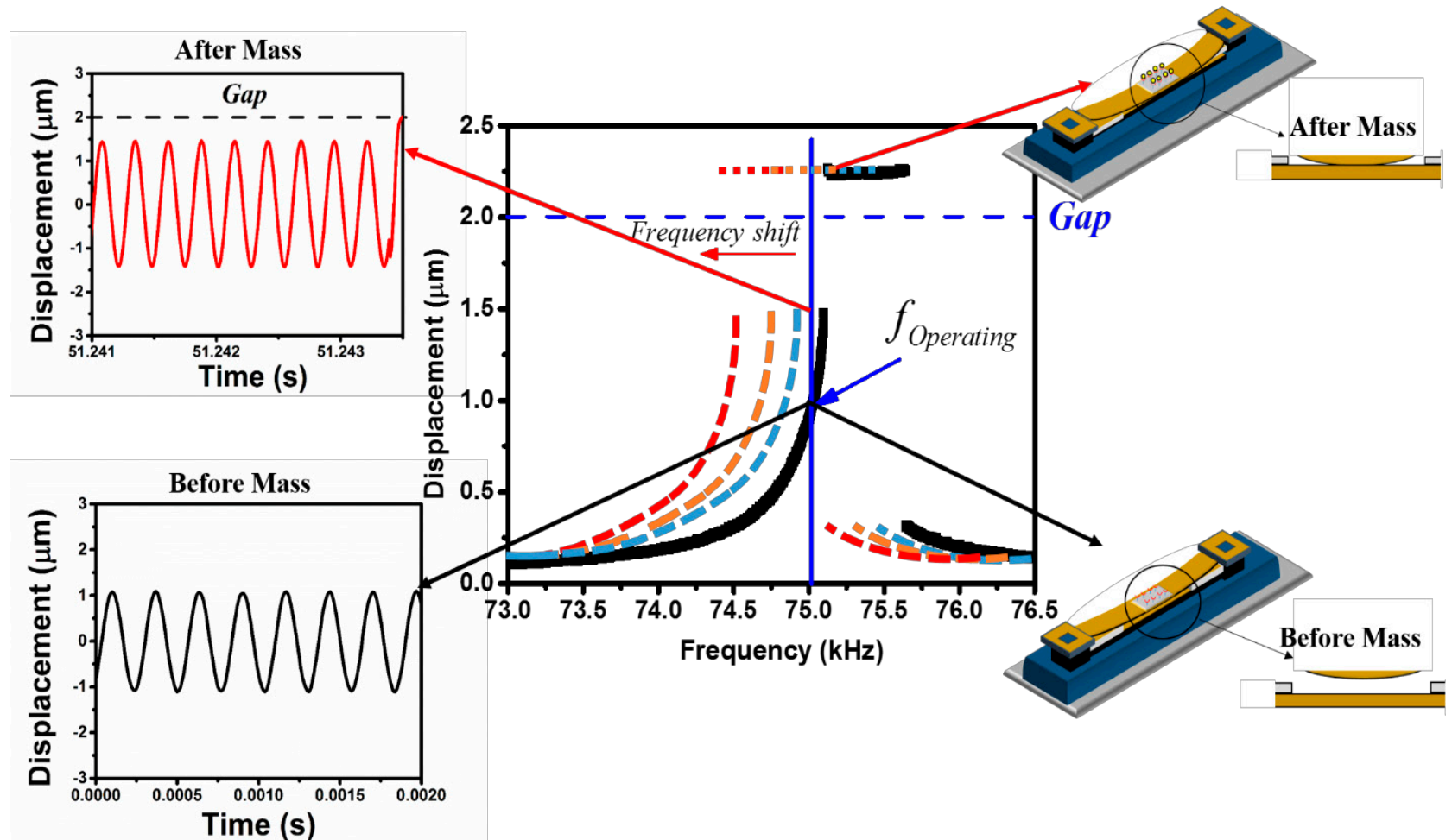
Switch  
Triggered by  
Mass



Before  
Mass

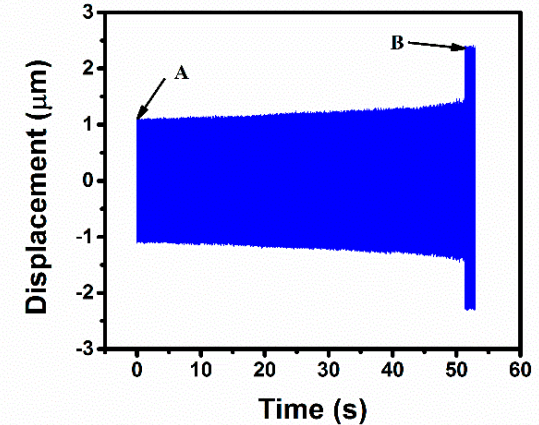
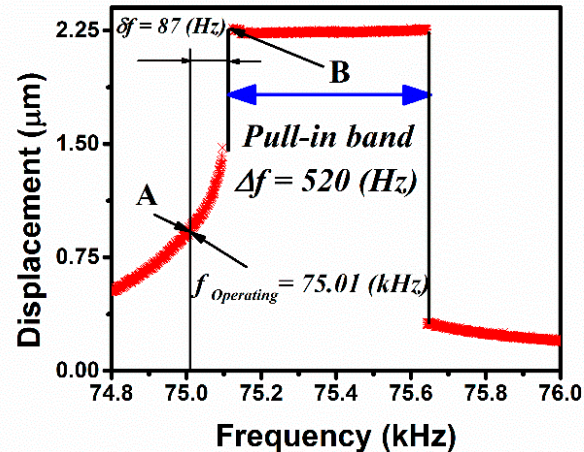
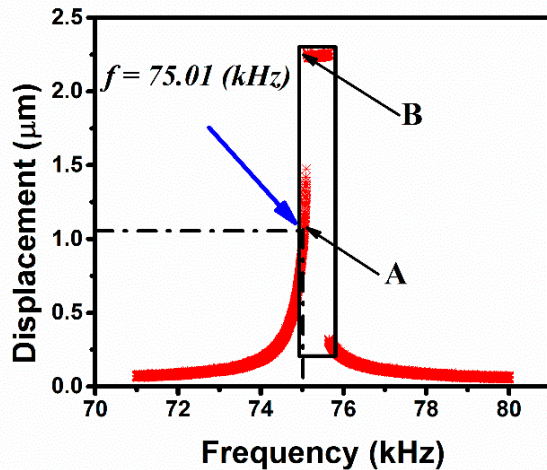


# Switch Triggered by Mass



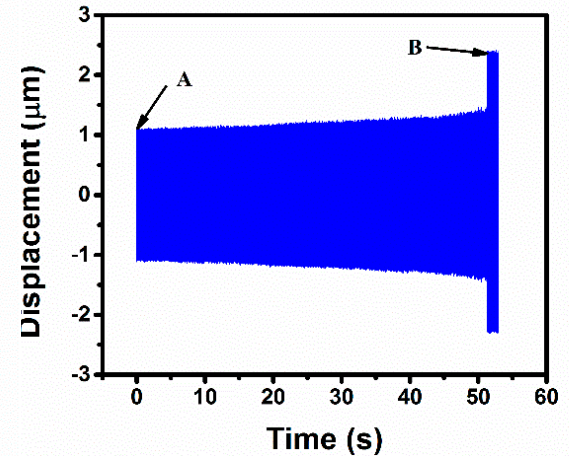
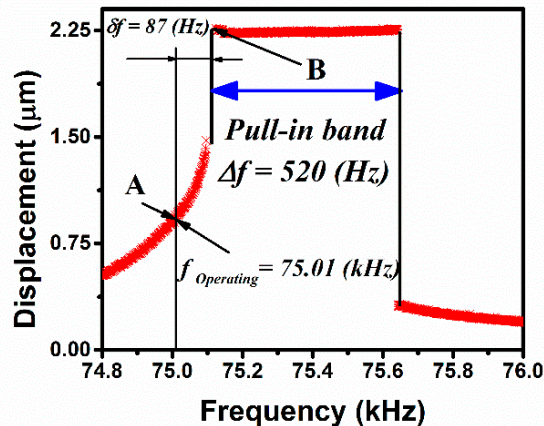
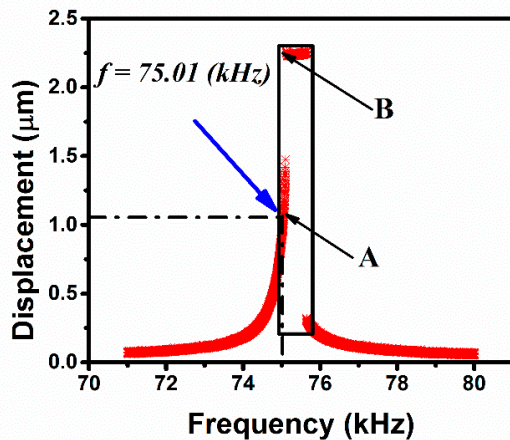
A Bouchaala, N Jaber, O Shekhah, V Chernikova, M Eddaoudi, MI Younis, "A smart microelectromechanical sensor and switch triggered by gas," Applied Physics Letters 109 (1), 013502, 2016.

# Switch Triggered by Mass



Time history of the midpoint displacement of the beam during vapor exposure.

- The figure shows the gradual increase of the midpoint displacement of the microbeam during the ethanol vapor exposure. This increase in displacement is due to the shift of the pull-in band toward the operating frequency.

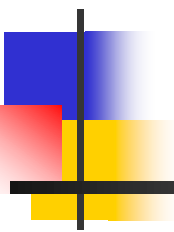


- The slope is  $|dY/df| = 3.95 \times 10^{-3} (\mu\text{m}/\text{Hz})$ .
- Based on the slope and the starting operating frequency, one can determine the frequency shift, and hence the absorbed mass, from the measured amplitude.
- The calculated frequency shift to reach pull in is  $\Delta f = 89.4 \text{ Hz}$  corresponding to an added mass threshold of  $\Delta m = 536 \text{ pg}$ .
- The actual measured value of  $87 \text{ Hz}$  (3% error).
- The added mass threshold can be controlled by shifting the operating frequency to lower or higher values. For example, to decrease the mass threshold value, the operating frequency can be moved closer to the pull-in band up to the limit the noise permits ( $\delta f_{\text{noise}} = 60 \text{ Hz}$ ).

# Summary and Conclusions Part I

- We demonstrated the advantage of using the nonlinear response of an electrostatically actuated resonator for gas sensing.
- The clamped-clamped microbeam is coated with HKUST-1 MOF, which is a very sensitive chemical layer.
- We demonstrated that frequency shift can be tracked in nonlinear regime using the linearly fitted upper branch in hardening behavior
- Two ideas of switches triggered by mass detection were demonstrated based on the jumps a resonator experiences in a hardening or a softening behavior.
- Switch triggered by mass detection based on dynamic pull-in, which eliminates the need for controllers, was demonstrated.

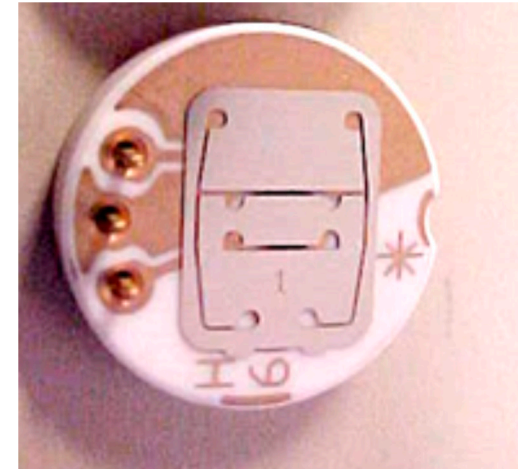
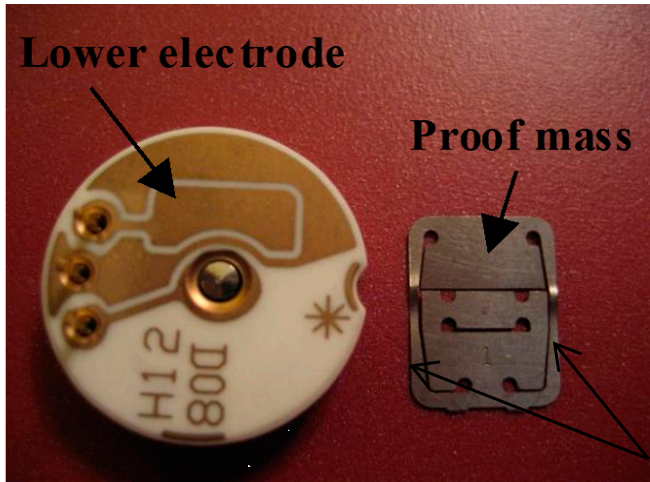
# Part II: Switch Trigger by Acceleration



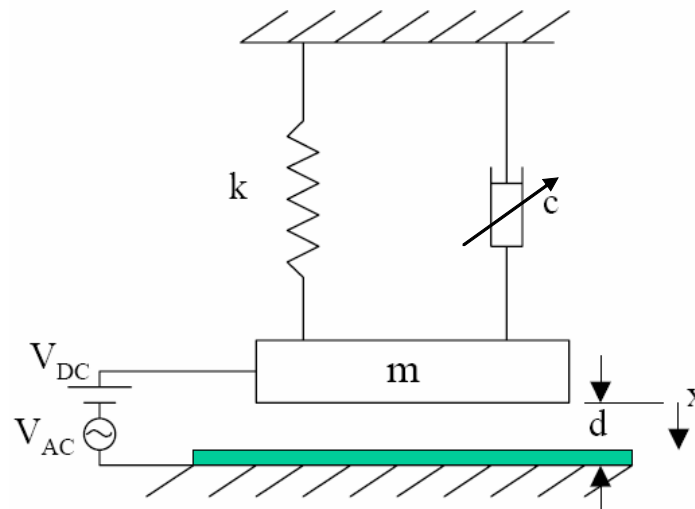
---

A new concept of switches (triggers) that are actuated at or beyond a specific level of mechanical shock or acceleration. The principle of operation of the switches is based on dynamic pull-in instability induced by the combined interaction between electrostatic and mechanical shock forces. These switches can be tuned to be activated at various shock and acceleration thresholds by adjusting the DC voltage bias.

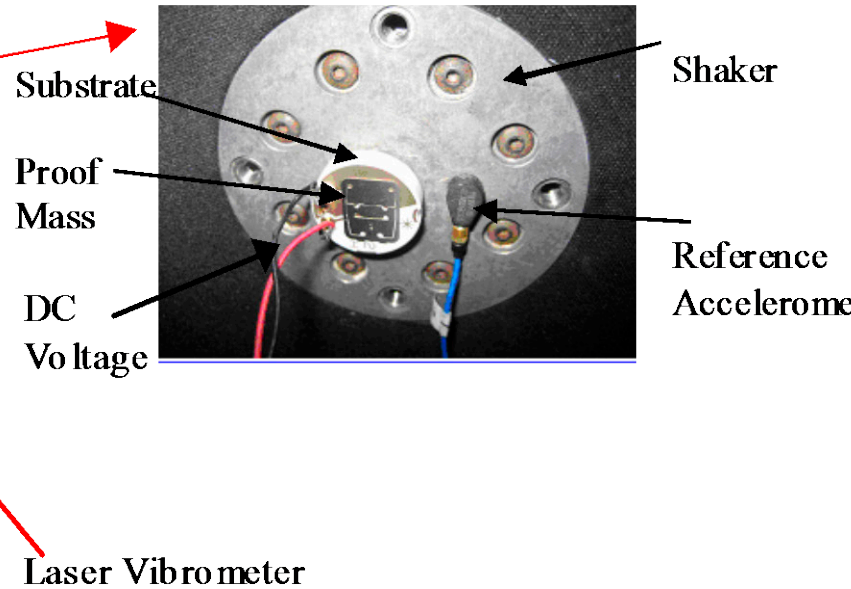
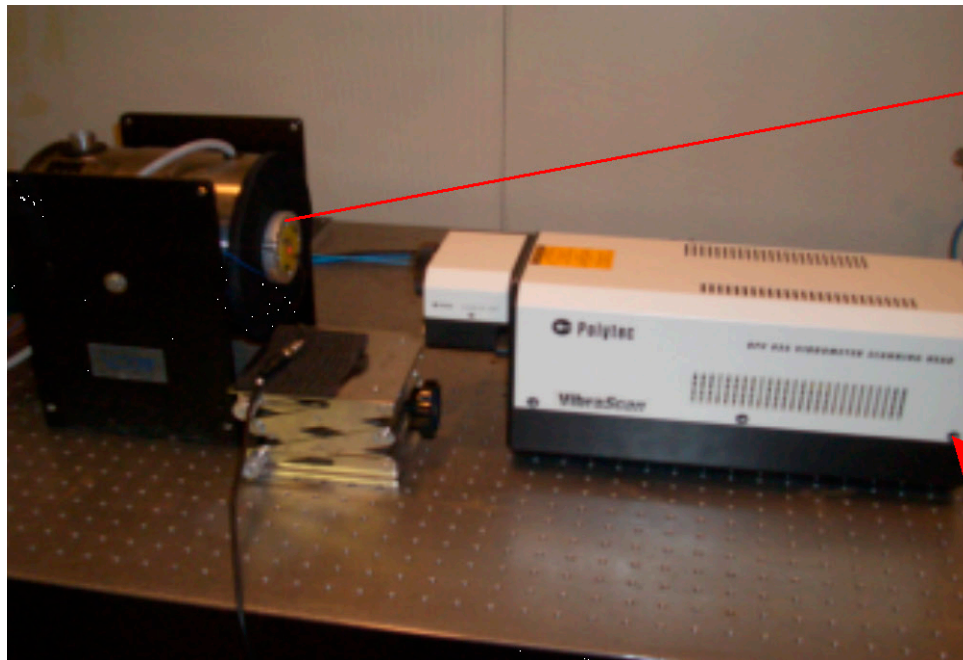
# The Device Under Investigation



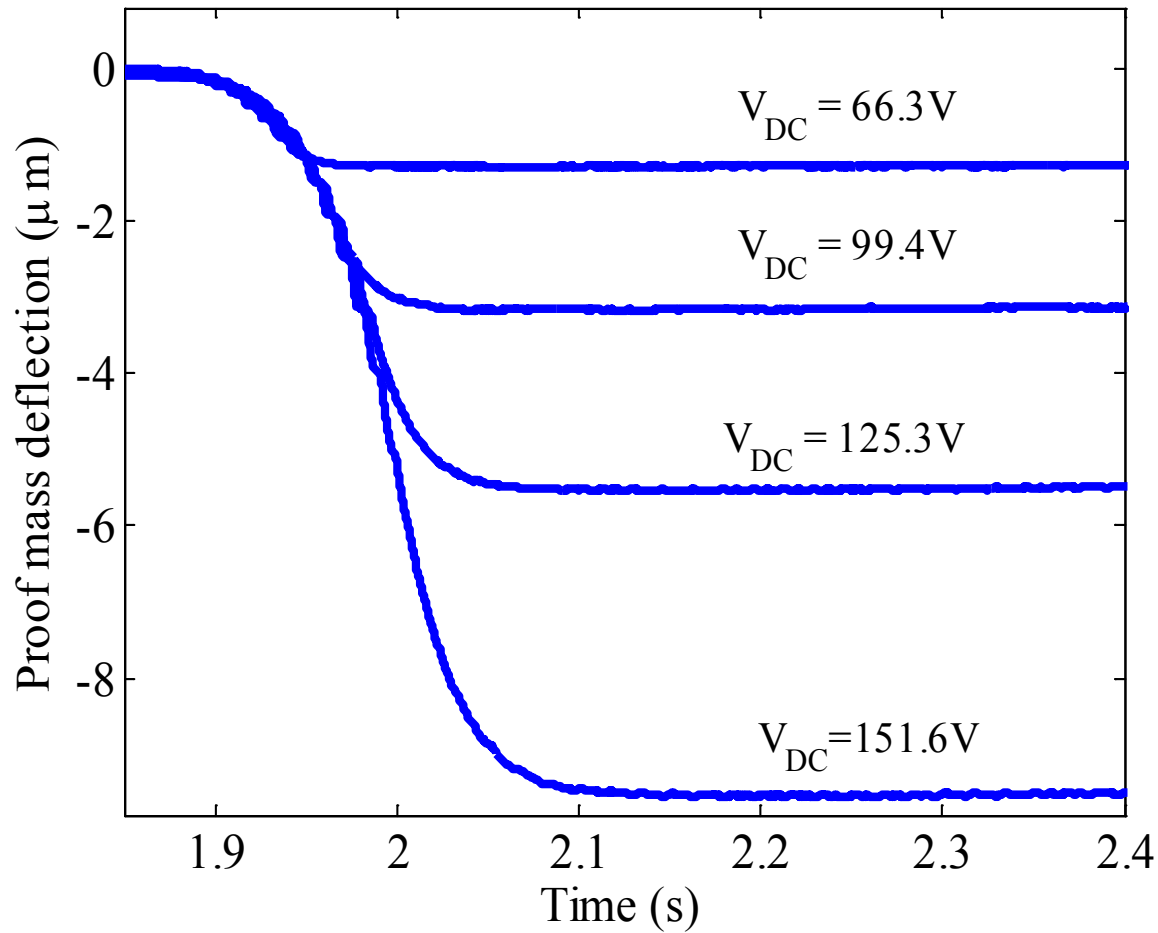
Sensata Technologies



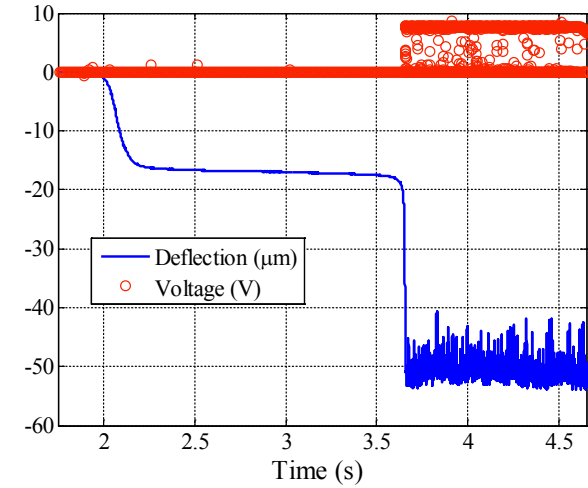
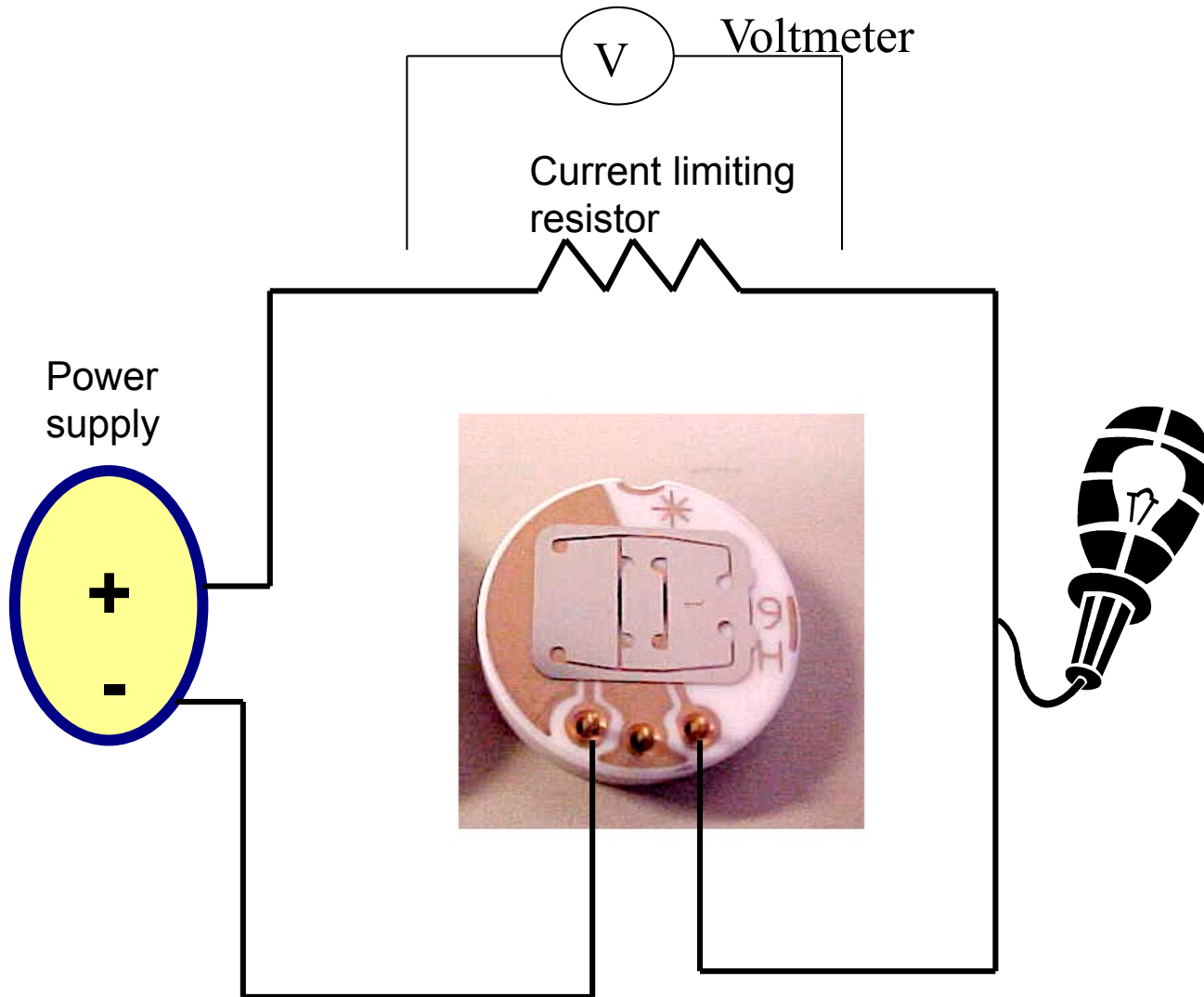
# Experimental Set up



# Response to DC Load

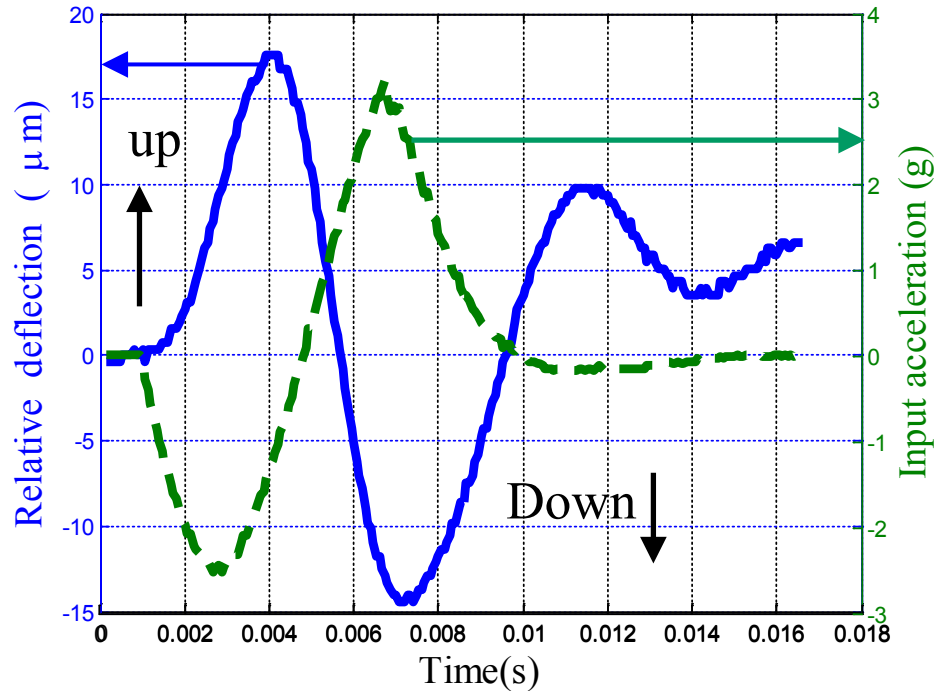


# Pull-in Detection

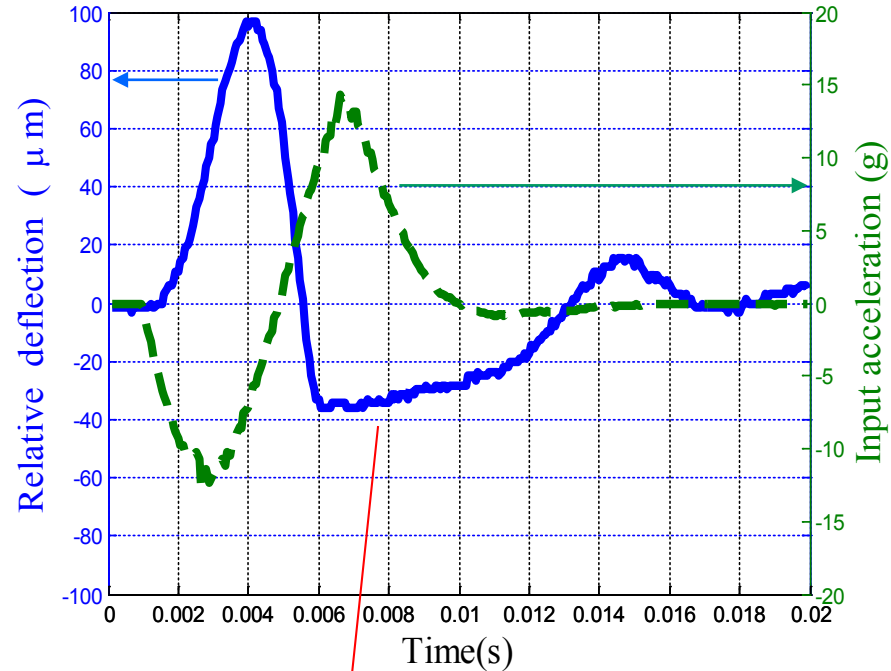
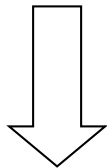


Small  
Lamp

# Response to Acceleration Pulses

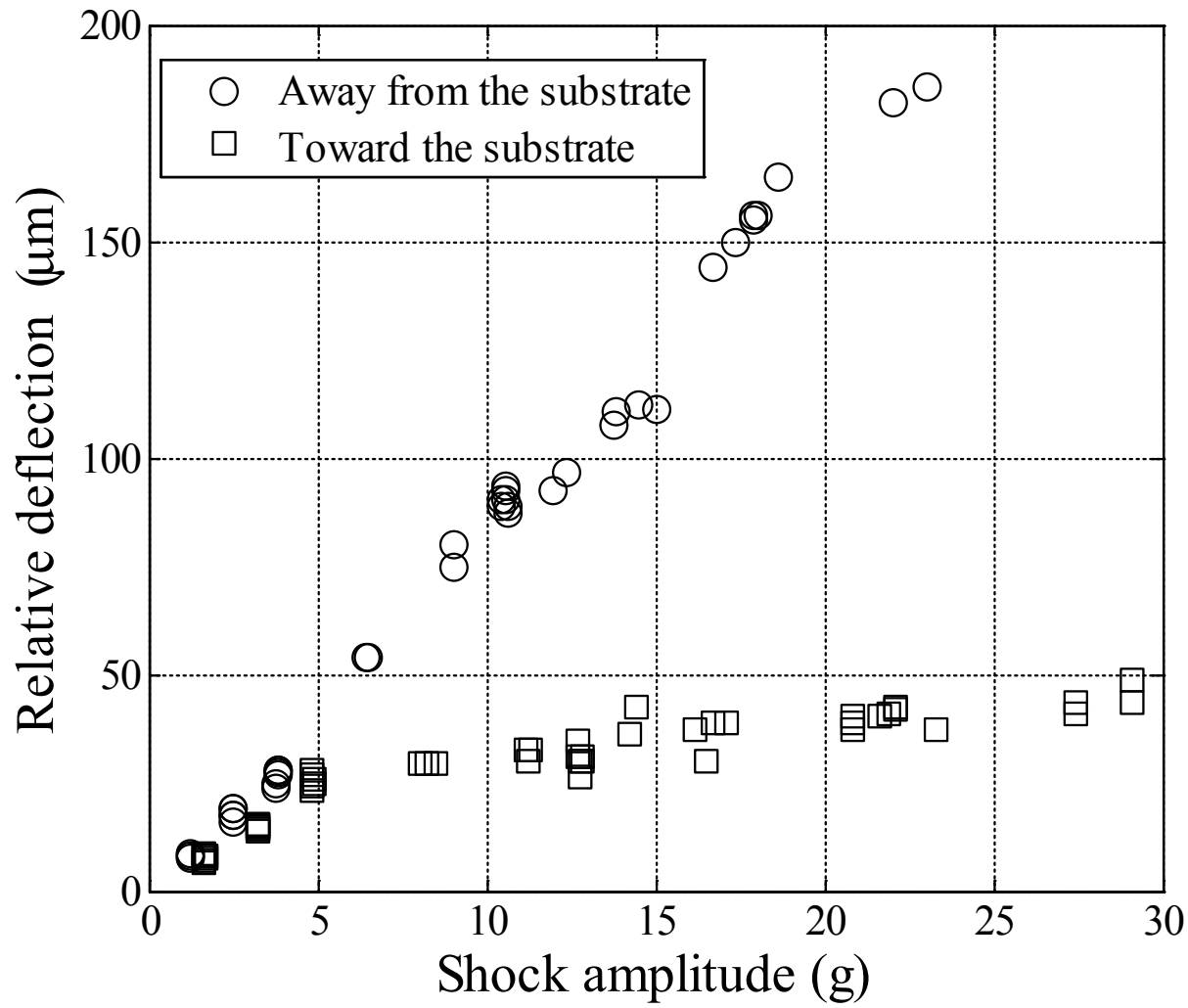


Toward  
substrate

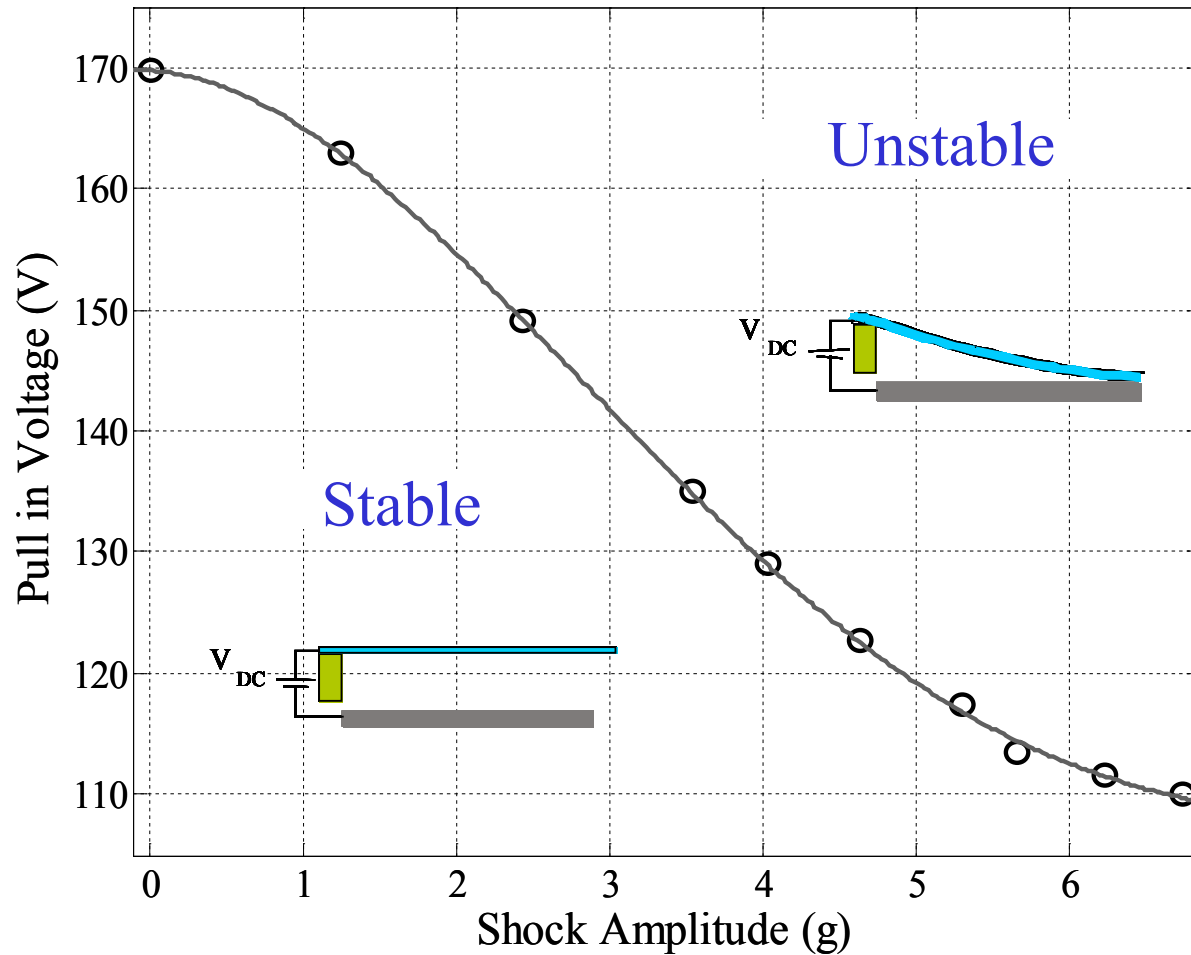


Close to substrate,  
squeeze-film damping  
is dominant

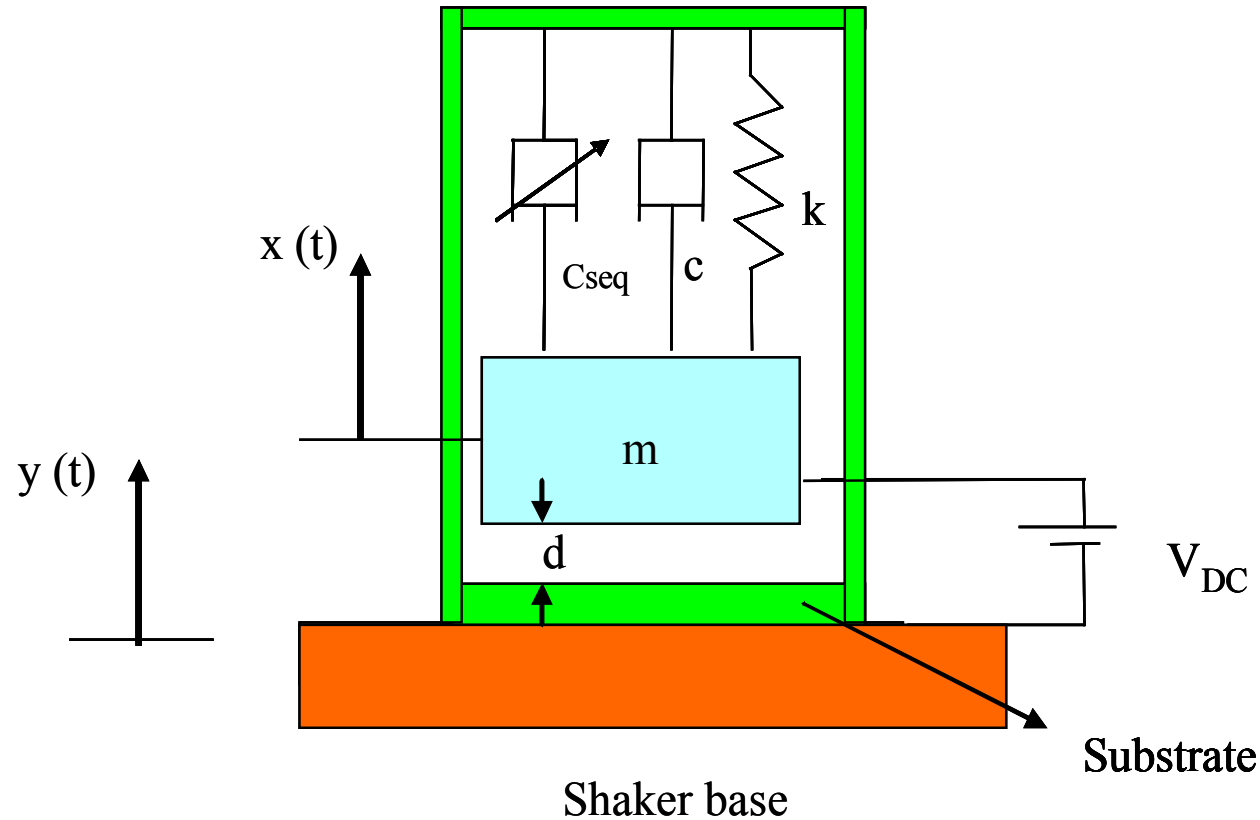
# Response to Acceleration Pulses



# Response to DC+ Acceleration Pulses

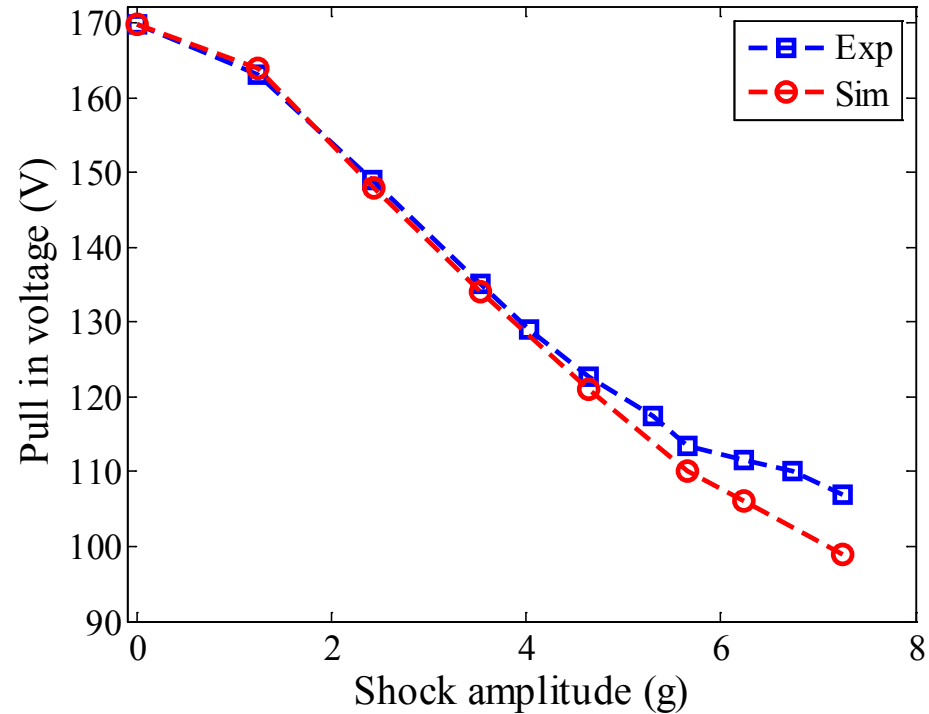
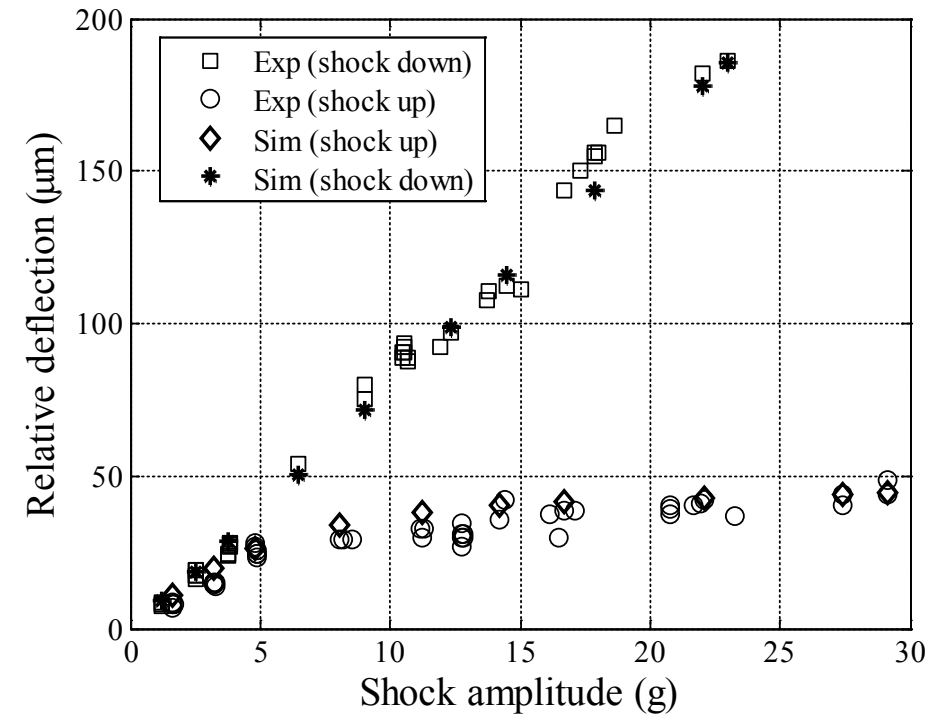


# CAS Model



$$m \ddot{z} + c \dot{z} + kz + f_{seq} = \frac{\epsilon A V_{DC}^2}{2(d+z)^2} - F_o m \ddot{y}$$

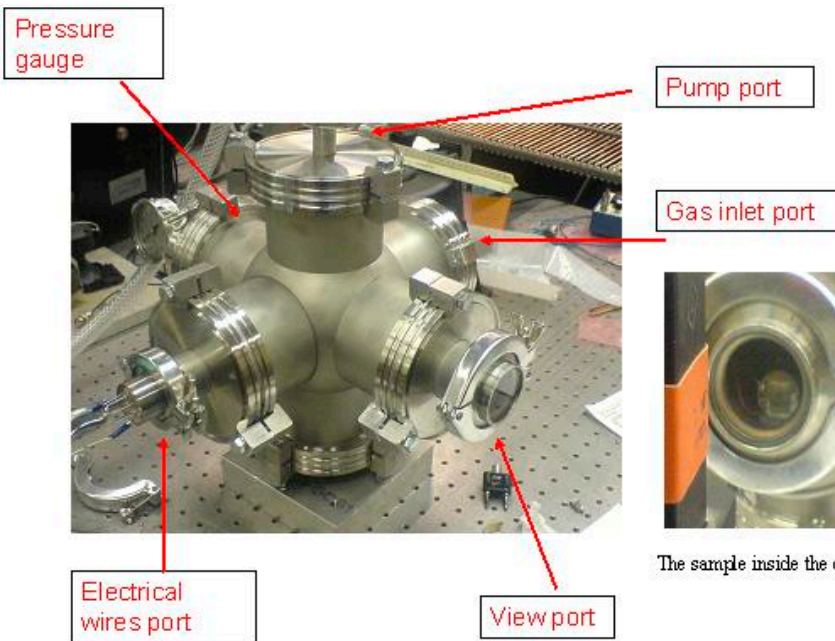
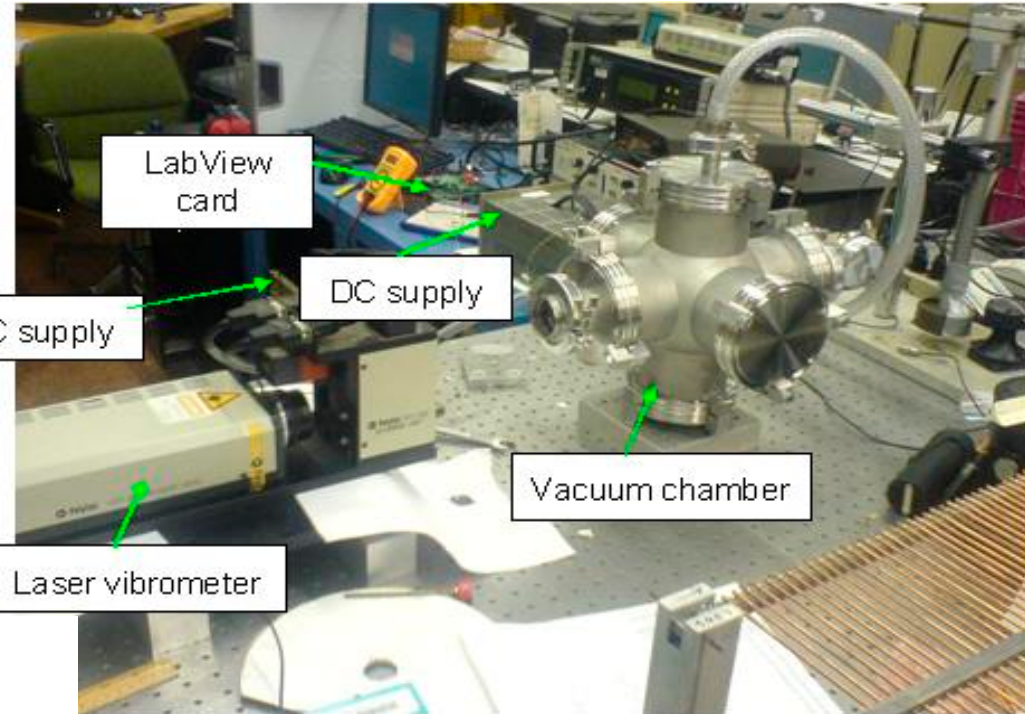
# Model Versus Experiment



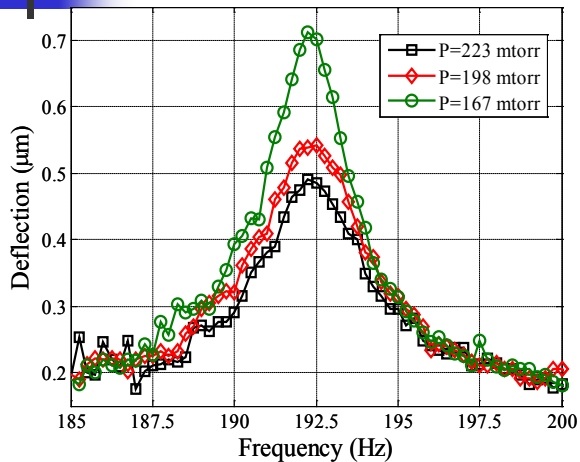
# Low-g Electrostatically Actuated Resonant Switch

- A new concept is presented of an electrostatically actuated resonant switch (EARS) for earthquake detection and low-g seismic applications.
- The resonator is designed to operate close to instability bands of frequency-response curves, where it is forced to collapse dynamically (pull-in) if operated within these bands.
- By careful tuning, the resonator can be made to enter the pull-in instability zone upon the detection of the earthquake signal, thereby snapping down as an electric switch. Such a switching action can be functionalized for alarming purposes or can be used to activate a network of sensors for seismic activity recording.

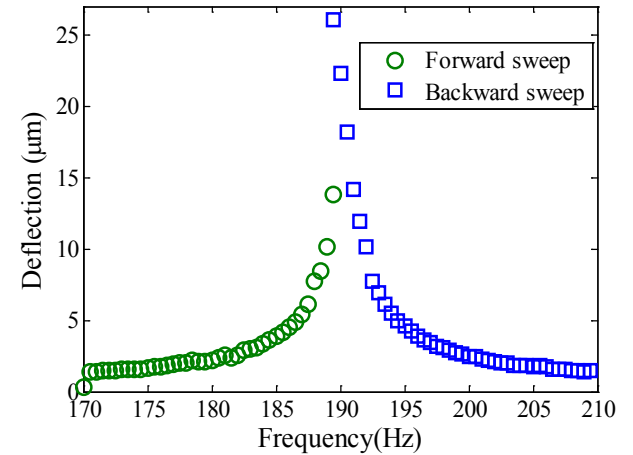
# Experimental Setup



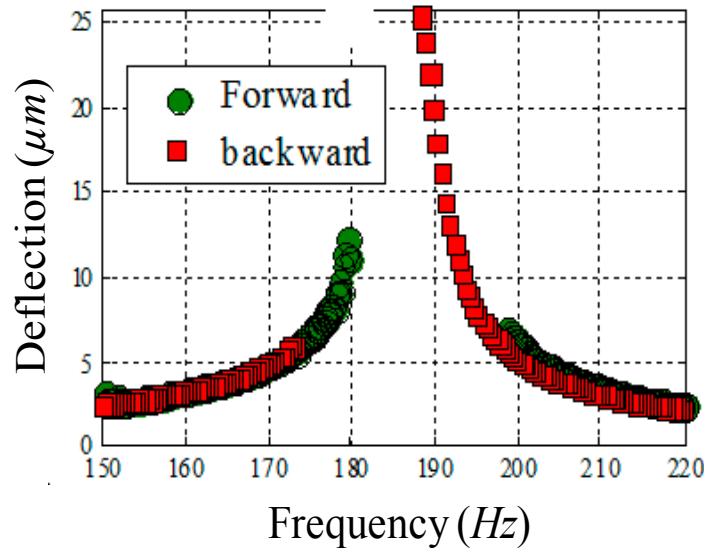
# Frequency Sweep Tests: Response to DC+AC Actuation



$$V_{DC} = 2 \text{ V and } V_{AC} = 4.2 \text{ V}$$

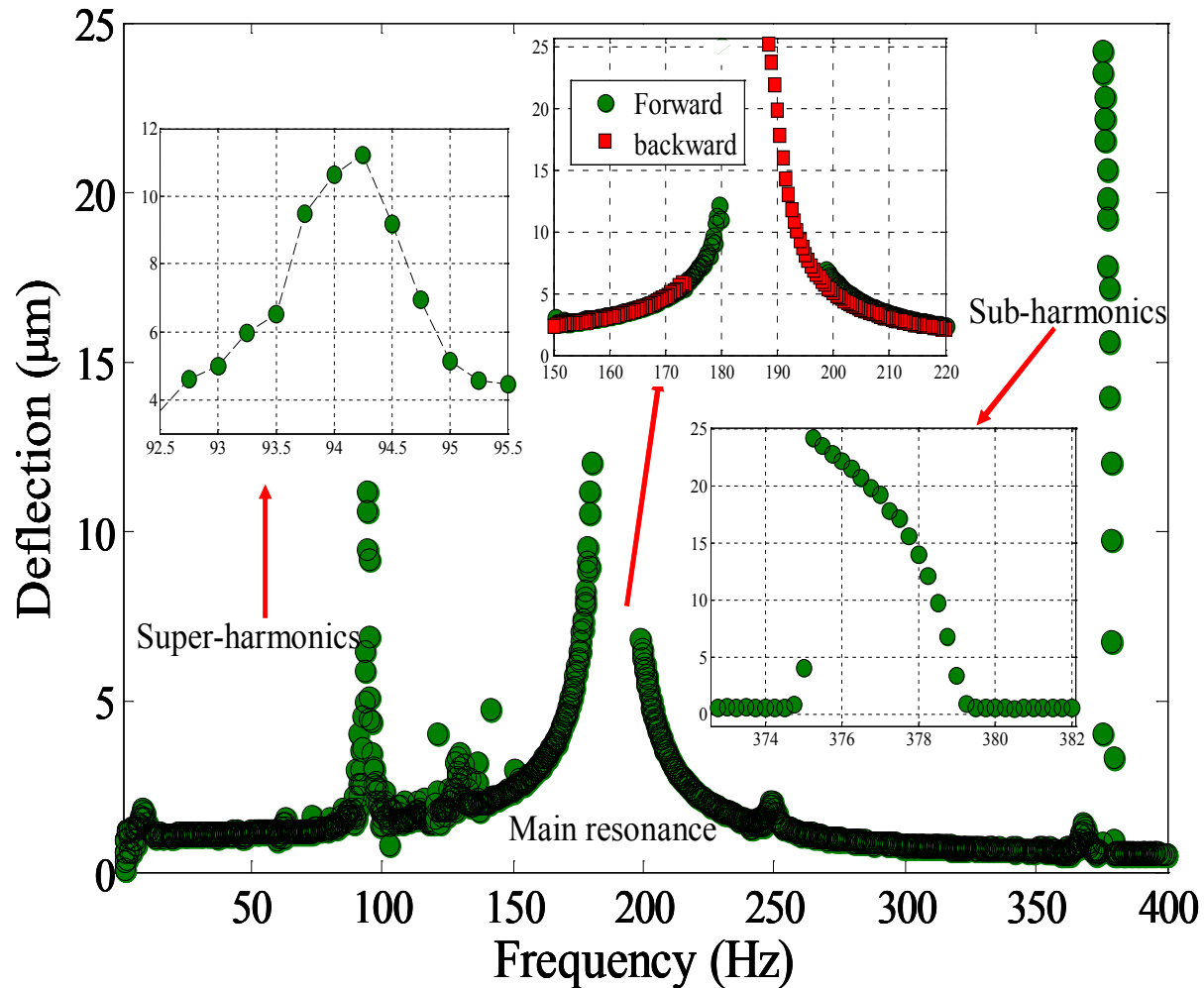


$$V_{DC} = 19.4 \text{ V and } V_{AC} = 15.3 \text{ V}$$



$$V_{DC} = 40.1 \text{ V and } V_{AC} = 18.4 \text{ V}$$

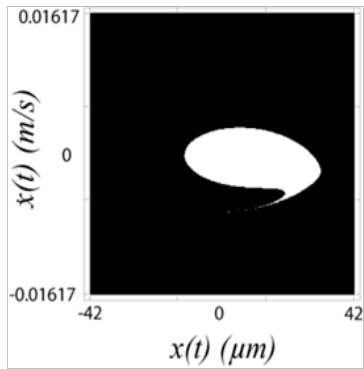
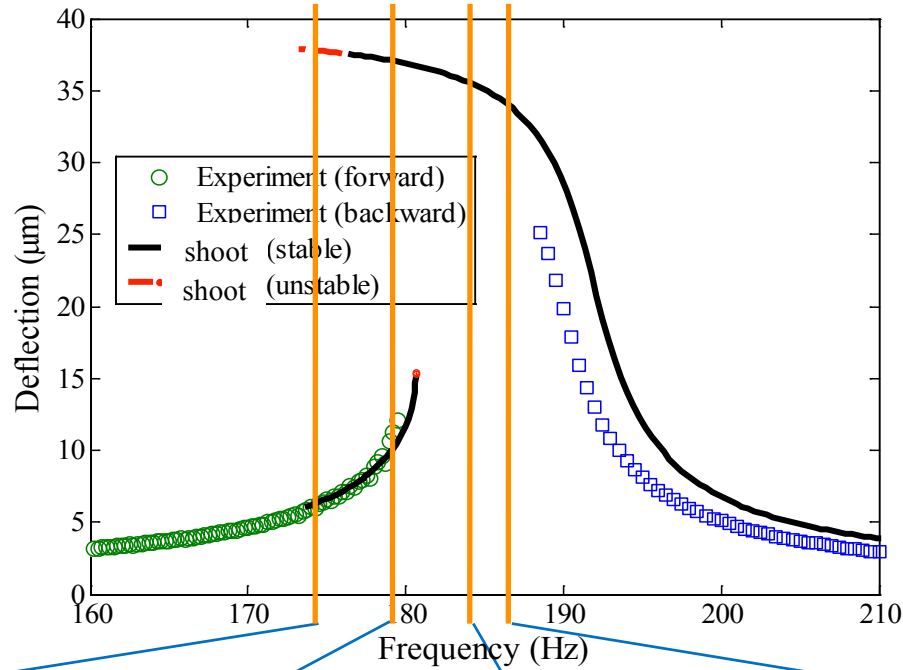
# Response to DC+AC Actuation



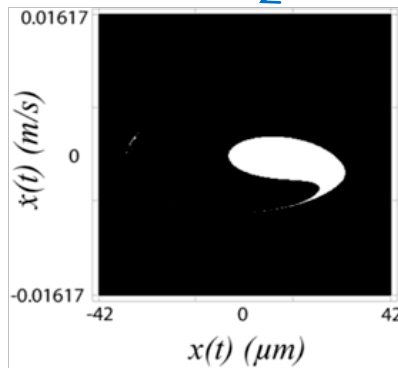
$$V_{DC} = 40.1 \text{ Volt}$$

$$V_{AC} = 18.4 \text{ Volt}$$

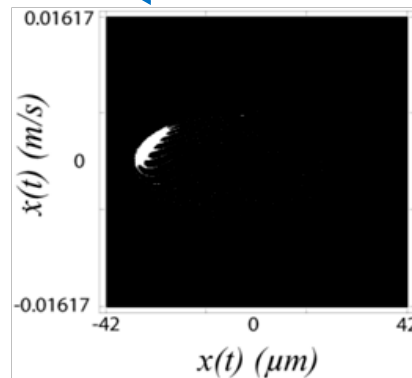
# Simulation Vs. Experiment



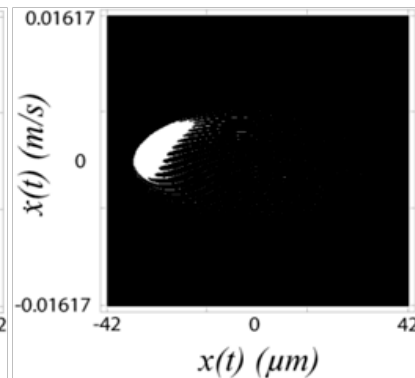
$\Omega = 174 \text{ Hz}$



$\Omega = 178 \text{ Hz}$

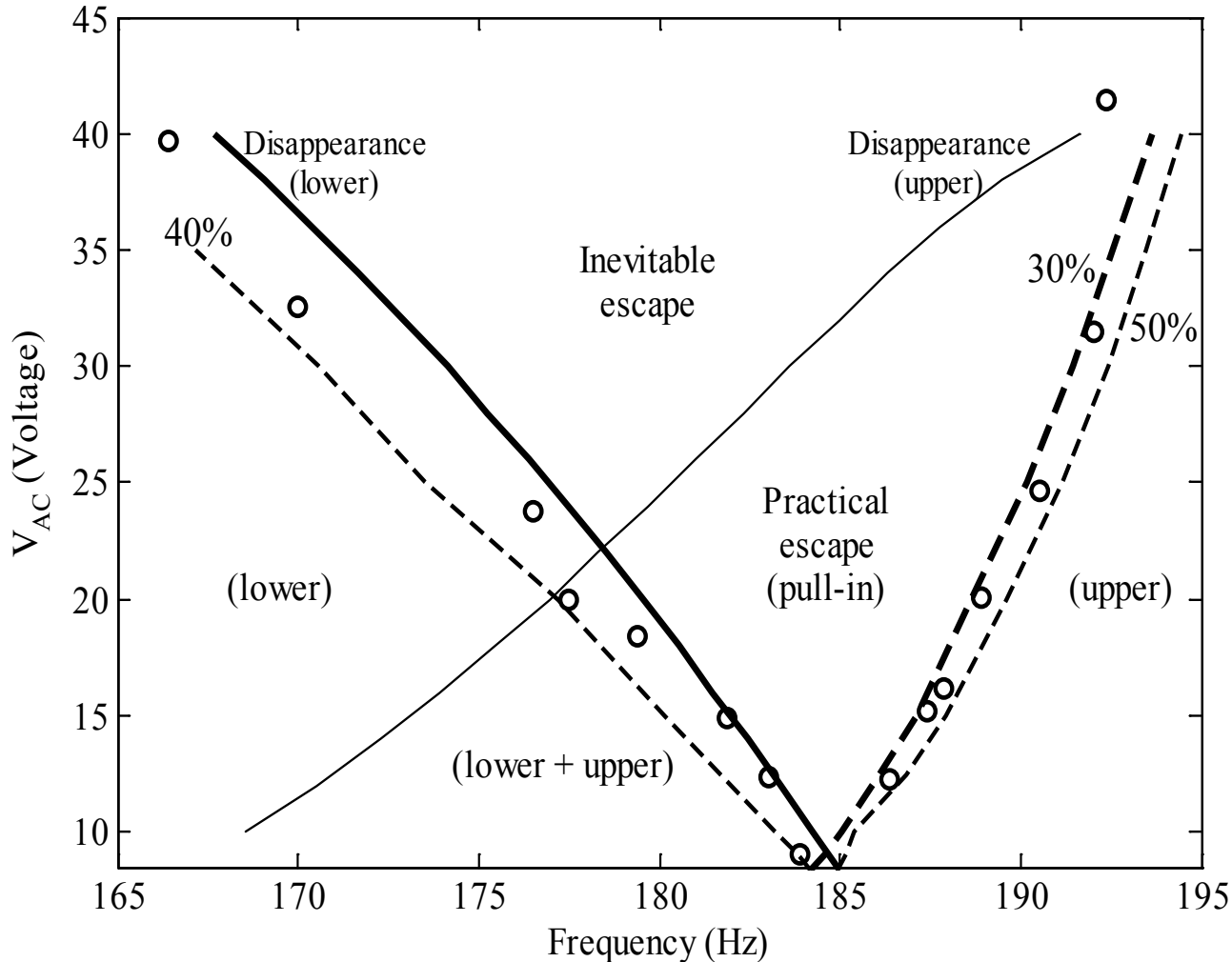


$\Omega = 184 \text{ Hz}$



$\Omega = 186 \text{ Hz}$

# Bifurcation Diagram



} %: Remaining  
 } fraction of the  
 } safe basin.

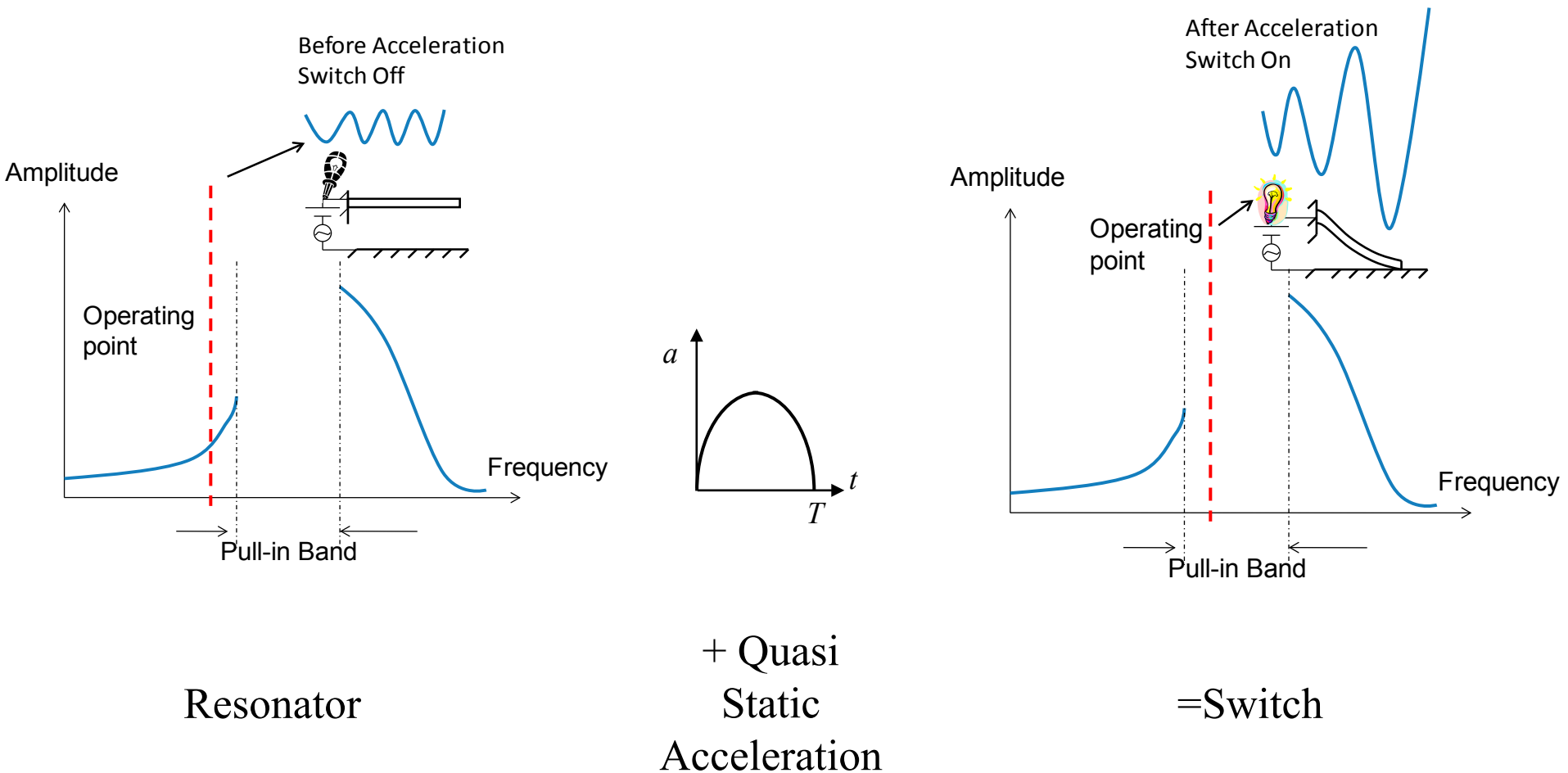
O: Experimental data

# Low-g Switch for Earthquake:



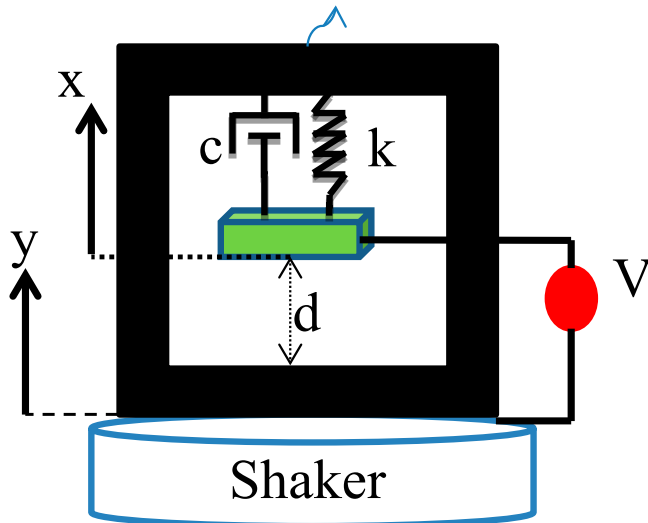
- In the event of earthquakes, immediate actions are required.
- Structural health monitoring: powering sensors when needed.

# Electrically Actuated Resonant Switch (EARS)

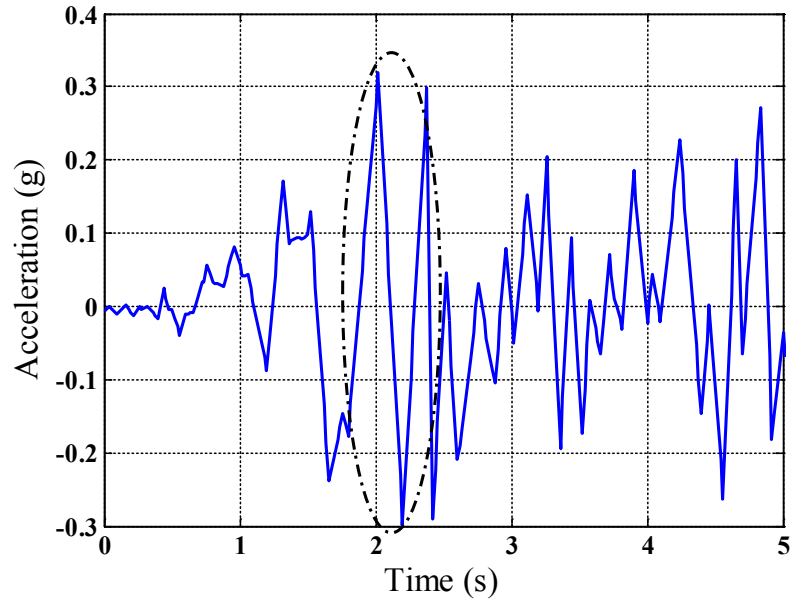


# The Model

Vacuum Chamber

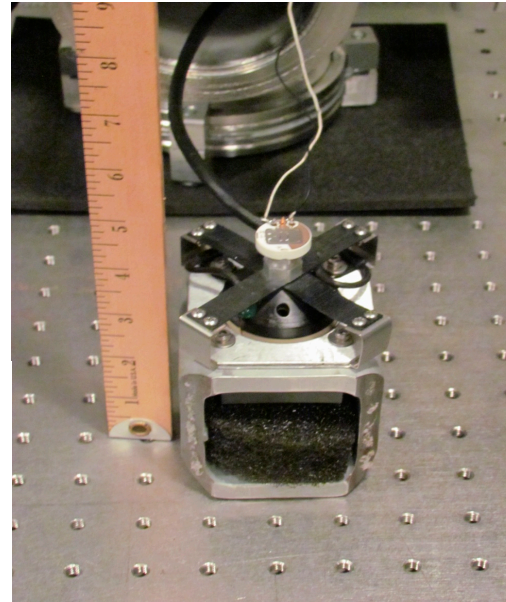
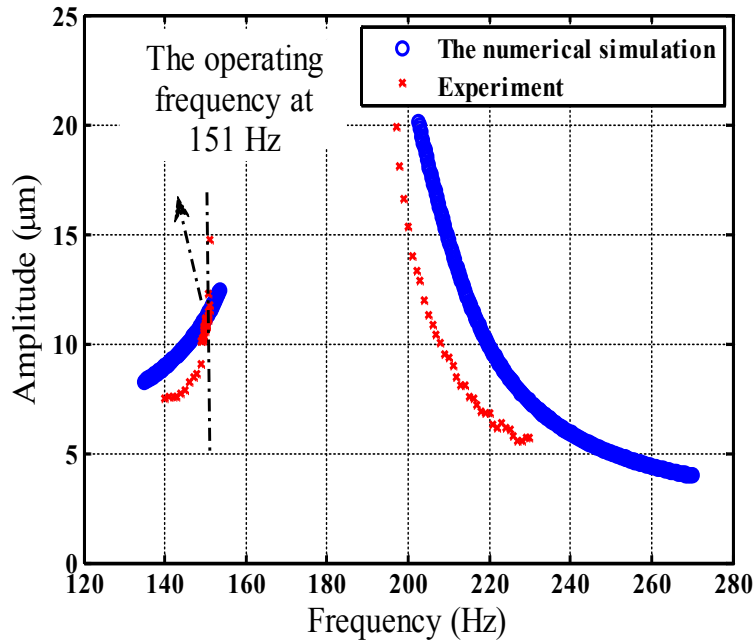


$$\ddot{z} + 2\omega\zeta\dot{z} + \omega^2 z = -\frac{\varepsilon A}{2m} \frac{(V_{DC} + V_{AC} \cos[2\pi\Omega t])^2}{(d+z)^2} - \ddot{y}$$

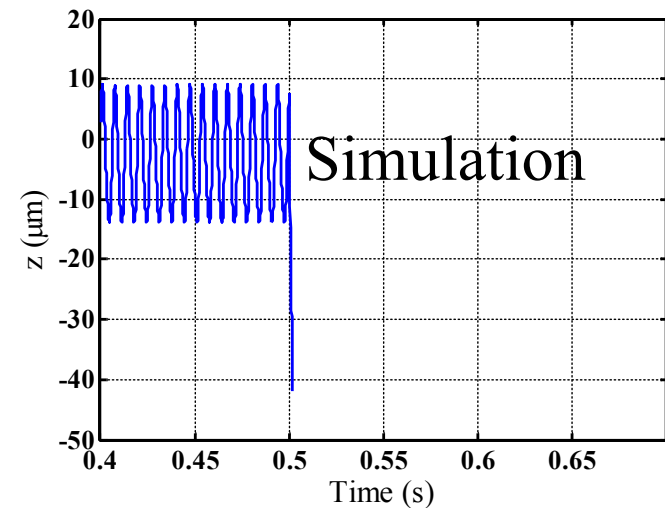
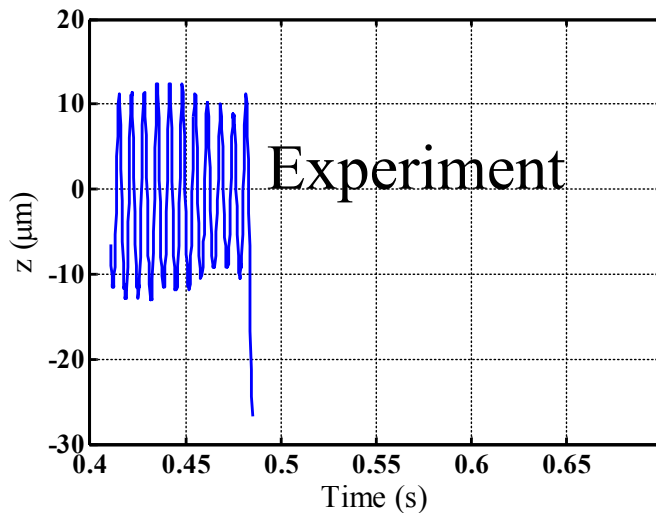
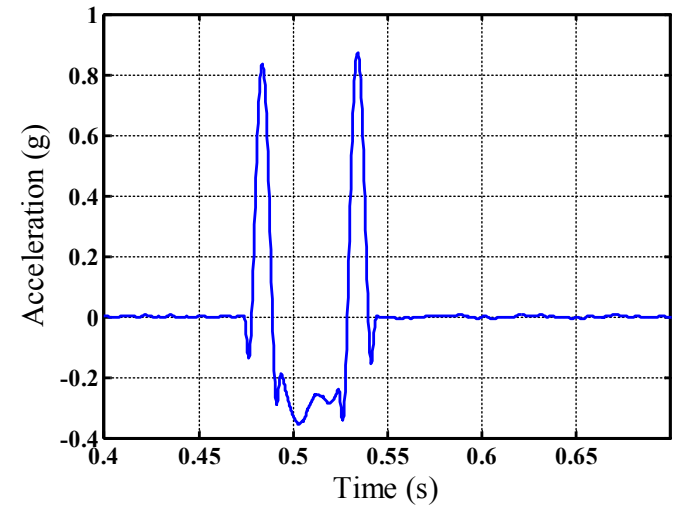
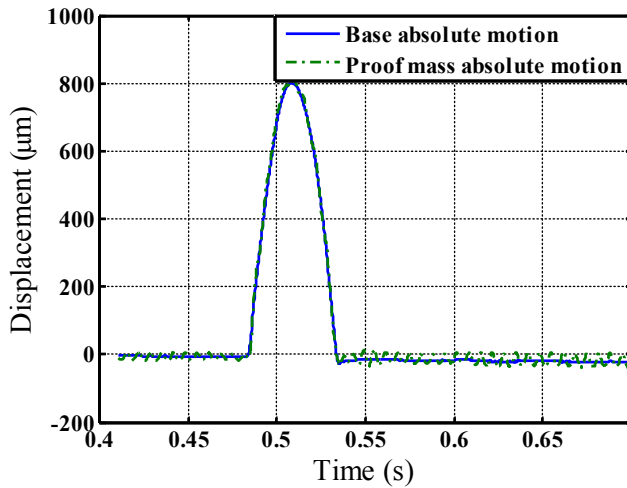


The El Centro Earthquake

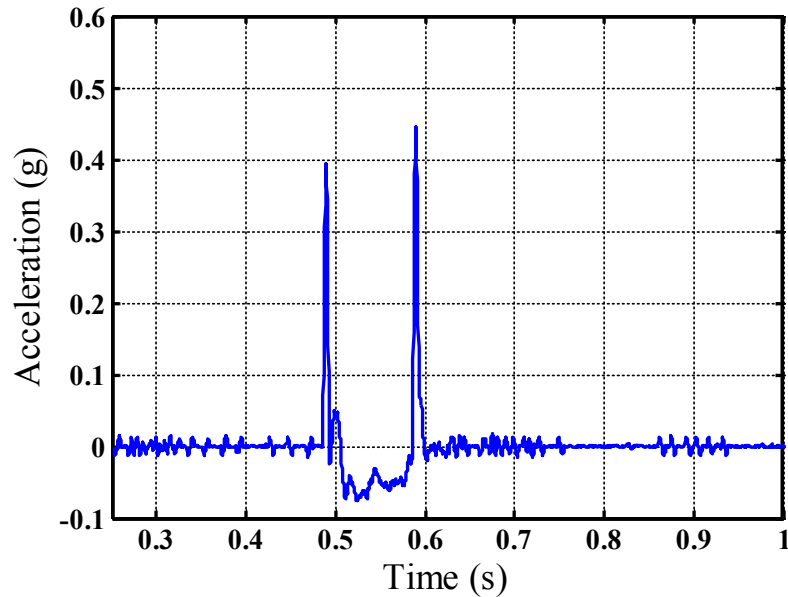
# Experimental Setup



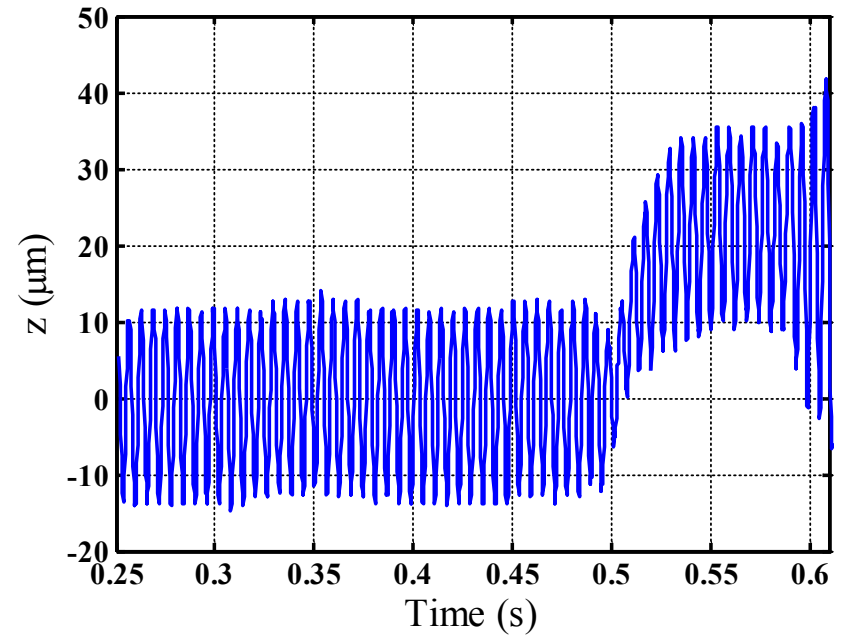
# Electrically Actuated Resonant Switch (EARS)



# Electrically Actuated Resonant Switch (EARS)



Input Pulse



Measured Response

- We presented experimental and theoretical investigation to the characteristics and performance of a new class of tunable threshold-acceleration switches actuated at or beyond a specific level of mechanical shock or acceleration.
- The exploitation of the dynamic pull-in instability of electrostatically actuated resonators to realize a sensor and an actuator at the same time has been demonstrated.
- The new concept of an electrostatically actuated resonant switch (EARS) for earthquake detection was validated numerically and experimentally, where measurements showed the EARS ability to switch due to a small amount of acceleration.
- The EARS concept could be useful in many applications to do switching action or to activate different devices.

Thank You